

Copyright
by
Chie Kozaki
2012

The Thesis Committee for Chie Kozaki
Certifies that this is the approved version of the following thesis:

Efficiency of Low Salinity Polymer Flooding in Sandstone Cores

APPROVED BY
SUPERVISING COMMITTEE:

Supervisor:

Kishore K. Mohanty

Co-supervisor:

Gary A. Pope

Efficiency of Low Salinity Polymer Flooding in Sandstone Cores

by

Chie Kozaki, B.S.

Thesis

Presented to the Faculty of the Graduate School of

The University of Texas at Austin

in Partial Fulfillment

of the Requirements

for the Degree of

Master of Science in Engineering

The University of Texas at Austin

May 2012

Dedication

To my loving parents and all my friends who have always supported me.

Acknowledgements

I would like to show my sincere gratitude to my advisor, Dr. Kishore K. Mohanty, whose encouragement, guidance and support from the initial to the final level enabled me to develop an understanding of the subject. I would also like to thank Dr. Gary A. Pope, for his inspired discussions and timely assistance throughout this work.

During this work I have collaborated with many colleagues for whom I have great regard and respect. I owe my deepest gratitude to Dr. Eric K. Dao, for his valuable advice and friendly help. His extensive discussions around my work and interesting explorations in operations have been very helpful for this study. I am also thankful to my colleagues, Gaurav Sharma, Peila Chen, Rahul Kumar, and Shashvat Doorwar for their friendship and constant help in my experimental work. This thesis would not have been possible without their support.

I also wish to thank Dr. Do Hoon Kim and Christopher Britton for always taking time to help me and answer my questions. I am grateful to Glen Baum and Gary Miscoe, who helped me to install experimental equipments. My sincere thanks go to Frankie L. Hart, Barbara D. Messmore, and Esther L. Barrientes for their administrative support. I would also like to thank all the other faculties and staff members at Petroleum Geosystems Engineering Department for making my time in graduate school so fulfilling and enjoyable.

I am truly indebted and thankful to my former supervisor, Dr. Nobuo Morita from Waseda University, who encouraged and supported me to have this opportunity to study at The University of Texas at Austin. He has always inspired me with his inquiring mind and great passion for research.

Lastly and most importantly, I wish to thank my parents, Keiko Kozaki and Yasuo Kozaki, for their patience, understanding, encouragement, and endless support throughout my life.

Abstract

Efficiency of Low Salinity Polymer Flooding in Sandstone Cores

Chie Kozaki, M.S.E.

The University of Texas at Austin, 2012

Supervisors: Kishore K. Mohanty and Gary A. Pope

Waterflooding has been used for many decades as a way of recovering oil from petroleum reservoirs. Historically the salinity of the injection water has not been regarded as a key variable in determining the amount of oil recovered. In recent years, however, evidence of increased oil recovery by injection of low salinity water has been observed in laboratories and fields. The technique is getting wider attention in the oil industry because it is more cost-effective than other EOR techniques.

The present work demonstrates the synergy of low salinity water flooding and polymer flooding in the laboratory scale. The use of low salinity polymer solution in polymer flooding has significant benefits because considerably lower amount of polymer is required to make the solution of a target viscosity. Low salinity polymer flooding can also increase oil recovery by lowering residual oil saturation and achieve faster oil recovery by improving sweep efficiency.

Several coreflood experiments were conducted to study the efficiency of low salinity water flooding and low salinity polymer flooding in mixed-wet Berea sandstone cores. All the core samples were aged with a crude oil at 90°C for 30-60 days before the

tests. All the polymer floods were conducted in the tertiary mode. A synthetic formation brine (33,800 ppm) was chosen for high salinity water and a NaCl brine (1,000 ppm) for low salinity water. Medium molecular weight HPAM polymer, FlopaamTM 3330S was used due to the low/moderate permeability of the Berea sandstone cores used in this study.

Coreflood tests indicate that injection of low salinity polymer solution reduces residual oil saturation by 5-10% over that of the high salinity waterflood. A part of the residual saturation reduction is due to low salinity and this reduction is achieved in less pore volumes of injection in the presence of polymers. Effluent ion analysis from both low salinity water flooding and low salinity polymer flooding showed a slight increase in divalent cation concentrations after the polymer breakthrough. Cation bridging may play a role in oil wettability and low salinity injection desorbs some of these cations.

Table of Contents

List of Tables	xi
List of Figures	xii
CHAPTER 1: INTRODUCTION	1
1.1 Motivation.....	1
1.2 Description of Chapters	3
CHAPTER 2: LITERATURE REVIEW	4
2.1 Overview	4
2.2 Early Salinity Studies.....	4
2.3 Wettability Studies.....	6
2.3.1 Wettability.....	6
2.3.2 Effect of Wettability on Petrophysical Properties	10
2.3.3 Effect of Brine Composition on Wettability	13
2.4 Low Salinity Studies	15
2.4.1 Mechanisms	15
2.4.2 Recent Work	19
2.5 Combined Low Salinity Studies	24
CHAPTER 3: MATERIALS, EQUIPMENTS, METHODOLOGY, AND DATA ANALYSIS.....	26
3.1 Materials	26
3.1.1 Aqueous Phases	26
3.1.2 Polymers	26
3.1.3 Crude Oil.....	27
3.1.4 Rocks.....	27
3.2 Experimental Equipments.....	28
3.2.1 Coreflood Experimental Equipments.....	28
3.2.2 Analytical Equipments.....	31
3.3 Methodology	32

3.3.1 Fluid Preparation.....	32
3.3.2 Core Preparation	33
3.3.3 Coreflood Description.....	33
3.4 Data Analysis	36
CHAPTER 4: RESULTS AND DISCUSSION.....	41
4.1 Low Salinity Water Flooding.....	41
4.2 Low Salinity Polymer Flooding in Semi-Tertiary Mode	59
4.3 Low Salinity Polymer Flooding in Tertiary Mode	67
CHAPTER 5: SUMMARY AND CONCLUSIONS	75
Appendix.....	79
References.....	86

List of Tables

Table 2-1: Relationship between Wettability and Common Measurements (Anderson, 1986)	10
Table 2-2: Conditions for Low Salinity Effects Listed by Austad <i>et al.</i> (2010)....	20
Table 3-1: Composition of Brines.....	26
Table 3-2: Report of Rock Mineralogy Analysis (weight%).....	27
Table 4-1: Berea A Core Properties.....	41
Table 4-2: Experiment 4.1 Fluid Properties at 85°C and 10s ⁻¹	42
Table 4-3: Berea B Core Properties	59
Table 4-4: Experiment 4.2 Fluid Properties at 85°C and 10s ⁻¹	60
Table 4-5: Berea C Core Properties	67
Table 5-1: End Point Relative Permeability of Experiment 4.1	77
Table 5-2: Results Summary of Experiment 4.1.....	77
Table 5-3: Results Summary of Experiment 4.2 and 4.3	77
Table A-1: Berea D Core Properties.....	79
Table A-2: Experiment A Fluid Properties at 85°C and 10s ⁻¹	79

List of Figures

Figure 2-1: Pore Scale Distribution of Fluids in the Rocks (Abdallah, 2007).....	7
Figure 2-2: Contact Angle Measurement (Abdallah, 2007)	8
Figure 2-3: Experimental Set-ups and Wettability Indices	9
Figure 2-4: Residual Oil Saturation vs. I_{a-h} for Berea Sandstone (Anderson, 2006)11	
Figure 2-5: Residual Oil Saturation vs. I_{a-h} for Other Sandstones (Anderson, 2006)11	
Figure 2-6: Effect of Wettability on Relative Permeability (Morrow <i>et al.</i> , 1973)12	
Figure 2-7: Role of Mobile Fines in COBR Systems (Tang and Morrow, 1999) .16	
Figure 2-8: Schematic of Oil & Clay (Lee <i>et al.</i> 2010)	17
Figure 2-9: The Number of Publications and Presentations Focused on Low Salinity Waterflooding (Morrow and Buckley, 2011)	19
Figure 2-10: Impact of Salinity on Electrical Double Layer (Lee <i>et al.</i> , 2010).....	22
Figure 2-11: Proposed Mechanism for Low Salinity EOR Effects (Austad <i>et al.</i> , 2010)	23
Figure 2-12: Effect of Salinity on Polymer Concentration (Ayirala <i>et al.</i> , 2010) .25	
Figure 3-1: Schematic of Coreflood Setup	30
Figure 4-1: Crude A Viscosity vs. Shear Rate ($T = 85^{\circ}\text{C}$).....	42
Figure 4-2: Experiment 4.1	43
Figure 4-3: Effluent Conductivity History (Tracer Test 1).....	44
Figure 4-4: Brine Drops on the Surface of Berea A	45
Figure 4-5: High Salinity Waterflood-1 Pressure Drop	46
Figure 4-6: High Salinity Waterflood-1 Oil Recovery	47
Figure 4-7: Low Salinity Waterflood-1 Pressure Drop.....	48
Figure 4-8: Low Salinity Waterflood-1 Oil Recovery	49

Figure 4-9: Tracer Test-2 Pressure Drop	50
Figure 4-10: Effluent Conductivity History (Tracer Test 2).....	50
Figure 4-11: High Salinity Waterflood-2 Pressure Drop	52
Figure 4-12: High Salinity Waterflood-2 Oil Recovery	53
Figure 4-13: Low Salinity Waterflood-2 Pressure Drop	54
Figure 4-14: Low Salinity Waterflood-2 Oil Recovery	55
Figure 4-15: Effluent Conductivity History (Tracer Test 3).....	56
Figure 4-16: Effluent Ion Concentration of High Salinity Waterflood 1	57
Figure 4-17: Effluent Ion Concentration of Low Salinity Waterflood 1	57
Figure 4-18: Effluent Ion Concentration of High Salinity Waterflood 2.....	58
Figure 4-19: Effluent Ion Concentration of Low Salinity Waterflood 2	58
Figure 4-20: Polymer Viscosity vs. Shear Rate (T = 85°C).....	60
Figure 4-21: Experiment 4.2	61
Figure 4-22: Effluent Conductivity History for Berea B (Tracer Test 1)	62
Figure 4-23: High Salinity Water – Low Salinity Polymer Flood Pressure Drop ..	64
Figure 4-24: High Salinity Water – Low Salinity Polymer Flood Oil Recovery ..	64
Figure 4-25: pH Profile of Experiment 4.2	66
Figure 4-26: Effluent Ion Concentration of Experiment 4.2.....	66
Figure 4-27: Experiment 4.3	68
Figure 4-28: Effluent Conductivity History for Berea C (Tracer Test 1)	69
Figure 4-29: High Salinity Water – Low Salinity Polymer Flood Pressure Drop ..	71
Figure 4-30: High Salinity Water – Low Salinity Polymer Flood Oil Recovery ..	71
Figure 4-31: pH Profile of Experiment 4.3	73
Figure 4-32: Effluent Ion Concentration of Experiment 4.3.....	73
Figure 4-33: Effluent Viscosity of Experiment 4.3	74

Figure 5-1: Oil Recovery Curves from Experiment 4.1	78
Figure 5-2: Oil Recovery Curves from Experiment 4.2 and 4.2.....	78
Figure A-1: Polymer Viscosity vs. Shear Rate ($T = 85^{\circ}\text{C}$).....	80
Figure A-2: Experiment A	80
Figure A-3: Effluent Conductivity History for Berea D (Tracer Test 1).....	81
Figure A-4: Low Salinity Polymer-II – Low Salinity Water Flood Pressure Drop	83
Figure A-5: Low Salinity Polymer-II – Low Salinity Water Flood Oil Recovery	83
Figure A-6: Effluent Ion Concentration of Experiment A.....	84
Figure A-7: End Point Effluent Viscosity of LSP-II Flood	85

CHAPTER 1: INTRODUCTION

1.1 MOTIVATION

The practice of waterflooding has been performed in oil fields for many decades mainly to maintain reservoir pressure and sweep oil towards the producing wells. Due to its simplicity and relatively low cost, waterflooding is still the most widely applied oil recovery technique in the fields even after the technical development of EOR processes such as gas injection and chemical injection.

For successful waterflood performance, it is essential to considerate numerous factors in waterflood design such as reservoir geology, reservoir and fluid properties, reservoir pressure, flow rate and timing of waterflood. Historically, the salinity of the injection water was not regarded as a key factor for efficient waterflooding and it was simply chosen so as to prevent the formation damage. However, numerous studies have reported that water composition can substantially affect oil recovery by waterflooding (Jadhunandan and Morrow, 1991, Yildiz and Morrow, 1996a, Tang and Morrow, 1997 Webb *et al.*, 2004, McGuire *et al.*, 2005, and Lager *et al.*, 2006). It was found that low salinity water has a potential for improving oil recovery in sandstone reservoirs. In practice, the composition of injection water is often different from the reservoir water depending on water availability. The possibility of improving waterflood recoveries through selection of the injection water, or changing the composition of the injection water during later stages of the flood, has obvious practical benefits.

Study of low salinity waterflooding was initiated by researchers at The University of Wyoming in the 1990's (Jadhunandan and Morrow, 1991, Yildiz and Morrow, 1996a and 1996b, Tang and Morrow, 1997). Ever since, growing number of publications have

proven the low salinity effects on oil recovery both in the laboratory and in the field. The general consensus among researchers is that injecting low salinity brine somehow creates a wetting state of the rock more favorable to oil recovery. Despite extensive research, however, the involved mechanisms of low salinity effects are not clearly identified as of yet due to the complexity of oil/brine/rock interactions. It is essential to understand the responsible mechanisms in order to optimize brine composition for waterflooding.

Even after the application of waterflooding, much oil usually remains in reservoirs. In some heterogeneous reservoir systems, as much as 70% of the original oil may remain. Thus, there is an enormous incentive for the development of other EOR techniques, aimed at recovering some portion of this remaining oil. Injection of polymer into reservoirs was first suggested in the early 1960s as a means of reducing mobility ratio by increasing injection water viscosity and also reducing the formation permeability. Since then, polymer flooding has been practiced by many operators to increase oil recovery. Recently, petroleum industry started showing growing interest in the possibility of further increasing oil recovery by combining the polymer injection technique and low salinity system, referred to as “low salinity polymer flooding”. Low salinity polymer flooding has a significant benefit because the use of low salinity water in polymer flooding process considerably reduces the amount of chemicals required. However, there have been few published studies devoted to the topic and there is a need for laboratory results from polymer injection.

The objectives of the present study are to investigate 1) the effectiveness of low salinity polymer flooding in Berea sandstone cores, and 2) the mechanism of low salinity effects in sandstone cores.

1.2 DESCRIPTION OF CHAPTERS

The outline for this thesis is as follows: Chapter 2 discusses literature related to the topic of this study. Chapter 3 introduces the experimental materials, equipments and experimental procedures used in this work. In chapter 4 experimental results are described and discussed. We summarize and conclude this thesis in Chapter 5.

CHAPTER 2: LITERATURE REVIEW

2.1 OVERVIEW

Waterflooding has been practiced for many decades as a way of maintaining pressure after primary depletion and recovering more oil. Historically, little consideration has been given to the effect of the injection brine salinity on the amount of oil recovered. Recent research, however, changed this preconception, and there is increasing evidence that injecting low salinity brines (<5000 ppm) has a significant impact on waterflood displacement efficiency in some sandstones.

This chapter presents the literature on low salinity waterflooding in sandstones both in the laboratory scale and the field scale. We begin with a discussion of early work and then move on to wettability study. Next, we discuss low salinity studies including the proposed mechanisms and the recent work. Finally, combined low salinity studies such as low salinity surfactant and low salinity polymer flooding in literature are reviewed.

2.2 EARLY SALINITY STUDIES

Researchers started testing waters of different salinity on core samples over half a century ago to study the water sensitivity effects on reservoir rocks. Here, reservoir sands that are susceptible to damage by exposure to waters are termed “water sensitive”.

Baptist and Sweeney (1954) injected three different salinities of water into four types of reservoir cores to study permeability variations and the water sensitivity of the sands. The samples were first flooded with toluene or benzene and dried at 105°C. After the air permeability was determined, the cores were saturated with NaCl brine (16,500 ppm) and liquid permeability was measured. The same procedure was repeated using

NaCl brine (8,250 ppm) and then distilled water. After all the floods, the samples were again dried and the final air permeability was measured. The amounts and type of clays in the samples were determined by X-ray diffraction analysis. The results of their experiments showed that water sensitivity increased with decreasing salinity and with decreasing permeability. Baptist and Sweeney also pointed out that the type and amount of clays present in the cores were key factors of the water sensitivity, and especially the sand containing kaolins, illites, and mixed-layer montmorillonite-illites was the most water sensitive.

Martin (1959) investigated the effect of clay hydration not only on permeability but also on oil recovery for the first time by injecting distilled water into the reservoir cores from Maracaibo Basin in Venezuela. Several core samples were treated with toluene to remove clay minerals while the rest of the samples were not treated. All the cores were flooded with heavy oil then oil was displaced with distilled water. The treated (clay-free) cores had lower residual water saturations and higher water relative permeabilities. The treated and untreated (clay-rich) cores had similar residual oil saturations and oil relative permeabilities. Martin suggested that in the clay-rich cores, the clay-water mixture was created and it was assumed to have higher apparent viscosities and lower water relative permeabilities than the clay-free water.

Bernard (1967) studied the effect of injection water salinity on oil recovery from cores containing hydratable clays. Either NaCl brine (from 1,000 ppm to 150,000 ppm) or distilled water was injected into sandpacks, Berea cores, and outcrop cores from Wyoming after initial oil saturations were established with Soltrol. The results showed that distilled water produced more oil than NaCl brines in all cases, accompanied by relatively high pressure drops across the cores. Bernard attributed the recovery increase to clay swelling and plugging of pore spaces available to oil and water.

General agreement among researchers at that point was that clays in the reservoir behaved differently towards water of different salinity. Several researchers proposed that it might raise the possibility of optimizing oil recovery by adjusting water salinity. However, due to the undesirably high pressure drop during floods caused by clay swelling, little attention was given to this topic for decades until Morrow *et al.* began their study.

2.3 WETTABILITY STUDIES

2.3.1 Wettability

Wettability is “the tendency of one fluid to spread on or adhere to a solid surface in the presence of a second fluid”. When the fluids are water and oil, the wettability is the tendency for the rock to preferentially imbibe oil, water, or both. The wettability of a rock is very important in oil recovery process because it controls the location, flow, and distribution of fluids within reservoir rocks (Anderson, 1986).

There have been several different degrees of wettability presented in the literature. A rock is water-wet if the aqueous phase is retained by capillary forces in the smaller pores and on the walls of the larger pores, and the oleic phase alternatively occupies the center of the larger pores and form globules that might extend over many pores (Fig.2-1). A rock can have a neutral wettability if there is no clear preference for one fluid or another. A rock is fractionally-wet if it is composed of different minerals, each with different surface chemistry and adsorption properties, which can lead to wettability variations within a single reservoir. A rock can have mixed wettability, which was first introduced by Salathiel in 1973. A mixed-wet rock has the oleic phase completely occupying the oil-wet large pores and the aqueous phase occupying the water-wet small

pores or different minerals within the same pore may be wet by different fluids. Lastly, a rock is oil-wet if the oleic phase occupies the small pores and coats the walls of the large pores while the aqueous phase occupies the center of the large pores (Fig.2-1). Jarrell *et al.* (2002), however, points out that all reservoirs that claim to be oil-wet are actually mixed-wet by definition because the oleic phase does not occupy the small pores.

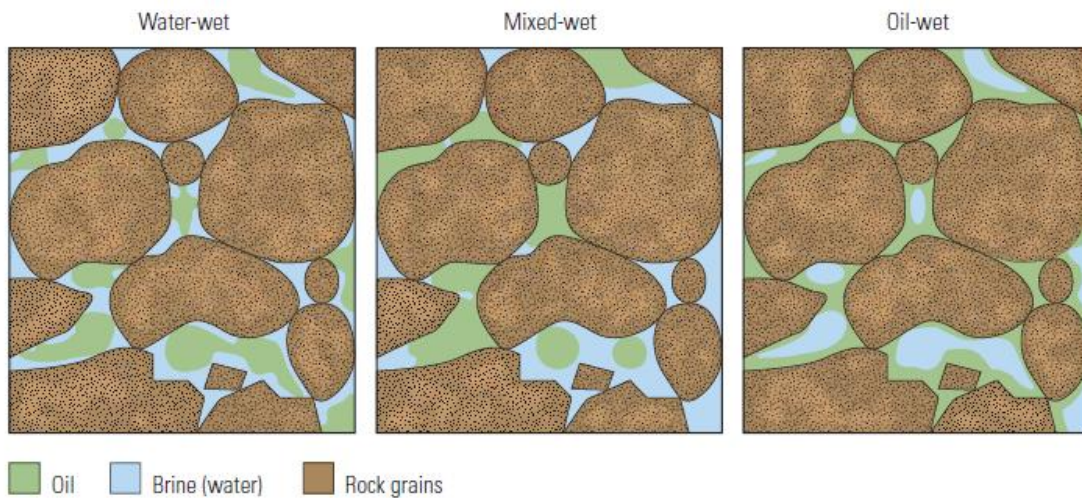


Figure 2-1: Pore Scale Distribution of Fluids in the Rocks (Abdallah, 2007)

Anderson (1986) reviewed the three major quantitative methods for determining wettability of a rock: the contact angle measurement, Amott method, and USBM method. The contact angle method only measures the wettability of a specific surface while Amott and USBM methods measure the average wettability of a core.

The contact angle is the best wettability measurement method when pure fluids and synthetic cores are used because there is no possibility of other compounds altering the wettability. The method is used to determine the effects of temperature, pressure, crude oil, and brine chemistry on wettability. In this method, the mineral surface is immersed in the water (or oil) and allowed to equilibrate. A drop of the oil (or water) is

then introduced on to the surface. The contact angle, θ , is then measured over time. Figure 2-2 illustrates the equilibrium contact angles for different wettability states. The magnitude of the contact angle gives a direct indication of the wettability of the rock.

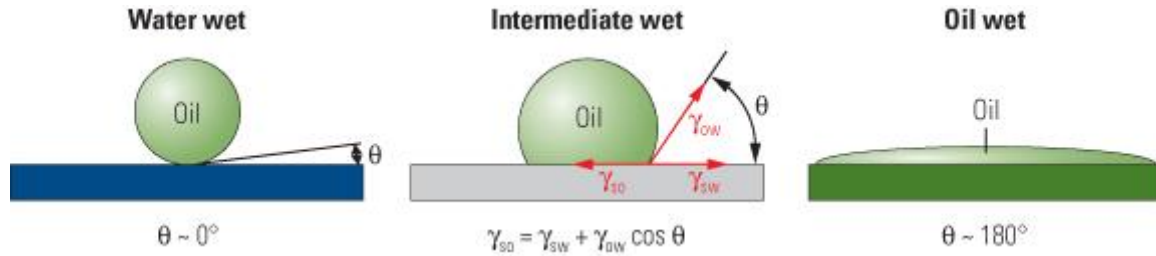


Figure 2-2: Contact Angle Measurement (Abdallah, 2007)

The Amott method was the first quantitative wettability measurement that could be used for rock cores. This method is based on the fact that wetting fluid will generally imbibe spontaneously into the core, displacing the non-wetting fluid. A centrifuge is used to further force the wetting fluid to imbibe more into the rock pore space, and hence forcefully displace the non-wetting fluid. Figure 2-3 shows the experimental set-up for the imbibition and centrifuge tests. In the Amott method, the core sample is first brought to residual water saturation S_1 by centrifuge with oil then subjected to the following tests: 1) spontaneous imbibition of water to reach S_2 and measure the volume of oil displaced spontaneously, 2) centrifuge the core with brine to residual oil saturation $1-S_4$ and measure the amount of oil displaced under the force, 3) spontaneous imbibition of oil to reach water saturation S_3 and measure the volume of water displaced spontaneously, 4) centrifuge the core with oil to reach residual water saturation S_1 and measure the amount of water displaced under the force. The results are expressed as a ratio of the volume displaced by spontaneous imbibition and the volume displaced by centrifuge, called

Amott index (Fig. 2-3). The Amott indices are dimensionless numbers that range from 0 to 1. The difference of the Amott indices is now commonly used as the modified wettability measure and is referred to as the Amott-Harvey index (Fig. 2-3). In this case, the wettability index will range from -1 to +1. Although the Amott method is a reliable measure of wettability of the core sample, its main drawback is that it is insensitive near neutral wettability since neither fluid will spontaneously imbibe and displace the other.

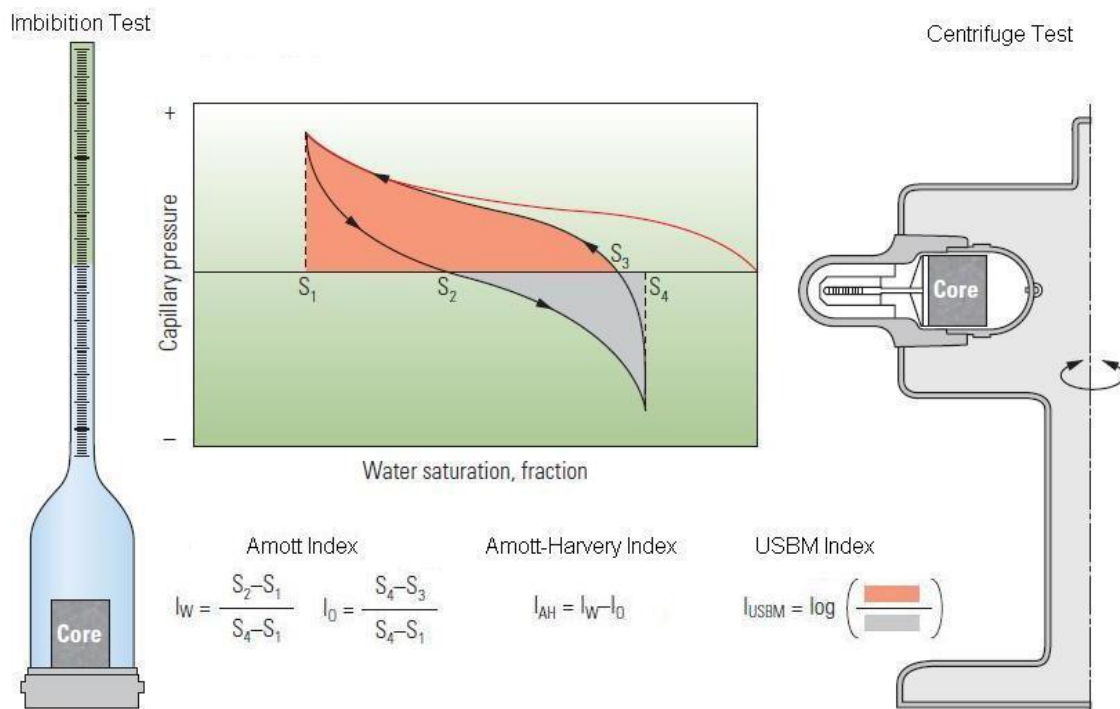


Figure 2-3: Experimental Set-ups and Wettability Indices

The third quantitative method is the USBM (United States Bureau of Mines) method, which was first introduced by Donaldson *et al.* (1969). In this method, the capillary pressure curve for each phase is generated using standard centrifuge method. Then the areas between each of the capillary pressure curves and the zero capillary

pressure line are calculated, and the logarithm of the ratio of the water-increasing to oil-increasing areas gives the USBM index (Fig. 2-3). The measurement range extend from $-\infty$ (strongly oil-wet) to $+\infty$ (strongly water-wet), although most measurement results are in a range of -1 to +1. The USBM index gives a measure of the energy needed to make the forced displacement, making them related but independent indicator of wettability while the Amott-Harvey index is based on the relative change in saturation. Table 2-1 provides the approximate relationship between wettability and common measurements.

Table 2-1: Relationship between Wettability and Common Measurements (Anderson, 1986)

		Water-wet	Neutral-wet	Oil-wet
Contact Angle	Min	0°	60° ~ 75°	105° ~ 120°
	Max	60° ~ 75°	105° ~ 120°	180°
Amott Wettability Index	I_w	>0	0	0
	I_o	0	0	>0
Amott-Harvey Wettability Index		$0.3 \leq I_{AH} \leq 1.0$	$-0.3 \leq I_{AH} \leq 0.3$	$-1.0 \leq I_{AH} \leq -0.3$
USBM Wettability Index		~ 1	~ 0	~ -1

2.3.2 Effect of Wettability on Petrophysical Properties

Several researchers have studied on the effect of wettability on residual oil saturation. Figures 2-4 and 2-5 show experimental data for Berea sandstone and for other sandstones respectively. From the figures, we can see that near neutral-wet or mixed-wet conditions give the lowest residual oil saturation. This finding indicates that residual oil saturation can be decreased and hence oil recovery can be increased by changing wettability.

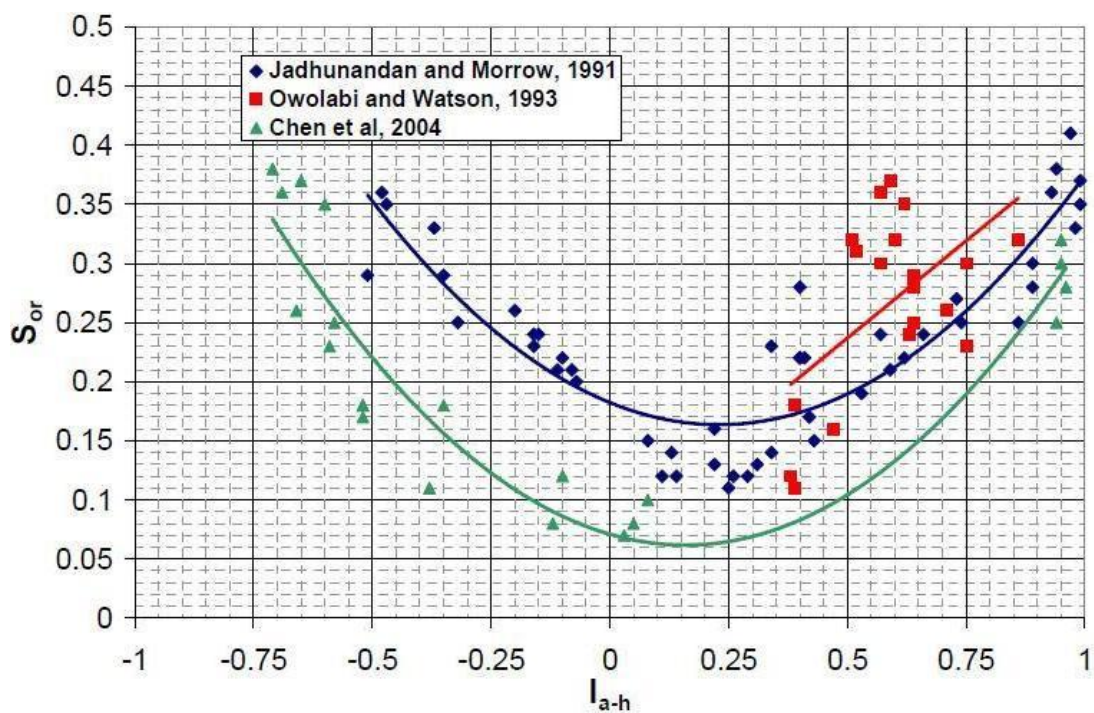


Figure 2-4: Residual Oil Saturation vs. I_{a-h} for Berea Sandstone (Anderson, 2006)

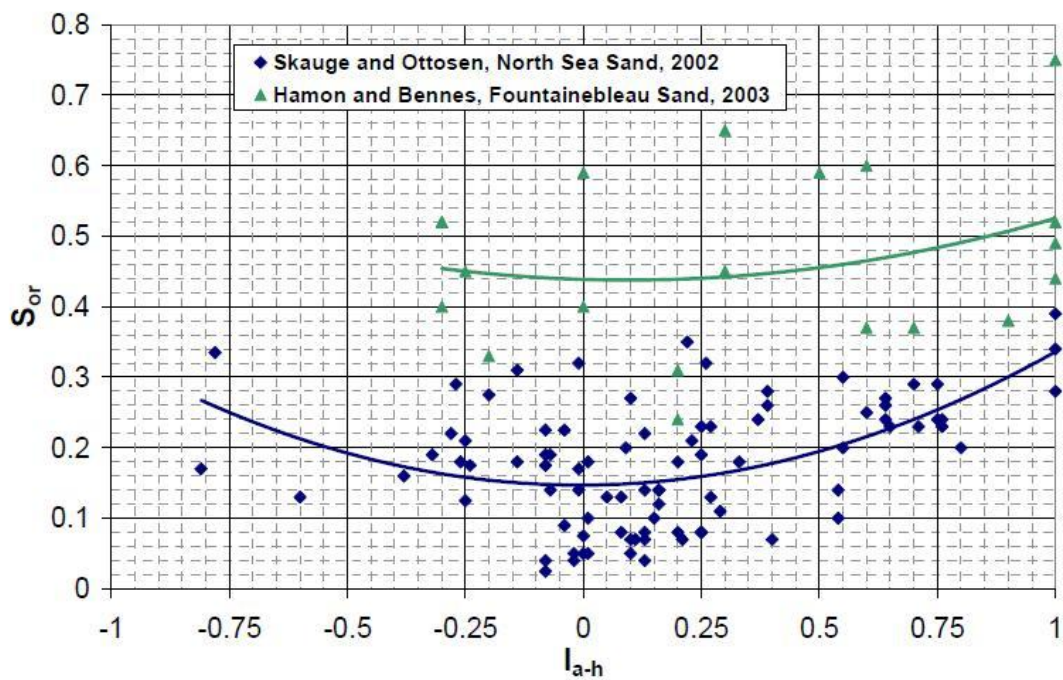


Figure 2-5: Residual Oil Saturation vs. I_{a-h} for Other Sandstones (Anderson, 2006)

The effect of wettability on relative permeability has also been investigated. Morrow *et al.* (1973) obtained relative permeability data for different wettability using Corey type functions (Fig. 2-6). There is an increase in the water relative permeability curve and a decrease in oil permeability curve when wettability shifts from water-wet to oil-wet. This effect is shifting the crossover point to lower water saturations.

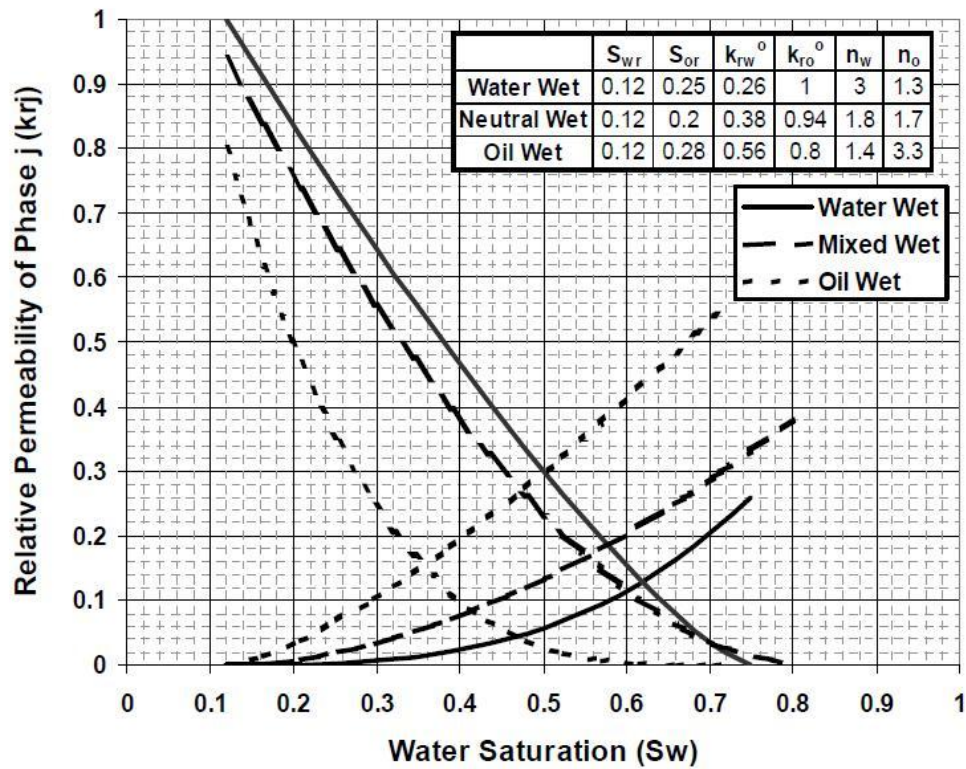


Figure 2-6: Effect of Wettability on Relative Permeability (Morrow *et al.*, 1973)

2.3.3 Effect of Brine Composition on Wettability

Rock wettability is highly dependent upon the surface chemistry and adsorption properties of the rock grains. Nearly all geologic formations are completely saturated with water during deposition and will be strongly water-wet initially. During hydrocarbon migration into the water-saturated formation, the rock can either remain water-wet or its wettability can change due to the interaction with the hydrocarbon. In the laboratory, different wettability state can be induced by exposing core samples to crude oil. This process is referred to as aging.

Jadhunandan and Morrow (1991) investigated the relationship between wettability and oil recovery by adjusting aging temperature, initial water saturation, and brine and oil composition. In their study, more than 50 waterfloods were performed on Berea sandstone cores with two crude oils (Moutray and ST-86) and several different salinities of brines composed of NaCl and/or CaCl₂. Wettability was measured by the Amott method after completing the coreflood. The waterflooding results showed a maximum in oil recovery at a wettability close to neutral ($I_{AH} \approx 0.2$). The results also showed that ST-86 oil was insensitive to brine composition and less sensitive to aging temperature and initial water saturation in terms of change in wettability while Moutray oil showed sensitivity to all parameters. Jadhunandan and Morrow (1991) concluded that aging temperature, initial water saturation, brine composition and crude oil were all significant factors in determining wettability of the crude-oil/brine/rock (COBR) system.

Morrow's research group began focusing more on the effect of brine composition on wettability and oil recovery. Yildiz and Morrow (1996a) performed waterflood on Berea sandstone cores using Moutray crude oil and two types of brines referred to as Brine 1 (4% NaCl + 0.5% CaCl₂) and Brine 2 (2% CaCl₂). The same brine was used throughout the coreflood in some cases and in the other cases the brine compositions was

changed one or more times during the flood. The results showed that when there is no change in brine composition, Brine 2 always gave higher oil recovery than Brine 1. The highest oil recoveries were observed when the cores had initial water saturation established with Brine 2 and they were flooded with Berea 1 and then Brine 2. Morrow *et al.* (1996b) also investigated the effect of brine composition on waterflood recoveries for Alaskan crude oil by using Brine 1 and Brine 2. For this oil, oil recovery was 15% higher for Brine 1 than for Brine 2 in waterflood with the identical connate and injection brines. From the results of these experiments, Morrow *et al.* concluded that brine composition could indeed affect the waterflood recovery of crude oil/brine/rock (COBR) systems. They also pointed out that wettability and oil recovery were strongly dependent on the specific crude oil and further experimental work with other crude oils was needed.

Tang and Morrow (1997) observed increase in oil recovery by waterflood with diluted brine. They conducted imbibition and waterflood tests on Berea sandstone cores using three crude oils from Dagang, Prudhoe Bay, and CS reservoirs, and three kinds of synthetic reservoir brines. Salinity of initial and/or injection brines was varied by changing the concentration by factors of 0.01, 0.1, and 2. Wettability of the core was characterized by examining the general form and relative positions of imbibition curves as well as the Amott index. From the results, they found that water wetness and oil recovery could be increased with dilution of both initial and injection brine or dilution of either. However the authors noted that because crude oil/brine/rock (COBR) interactions had the great complexity and specificity, it is necessary to test specific reservoir conditions rather than simply generalize. Based on these findings, researchers began focusing on possibility of low salinity waterflooding to improve oil recovery and analyzing the mechanism(s).

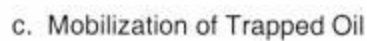
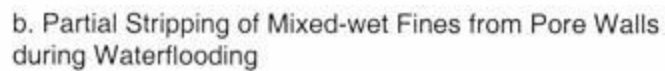
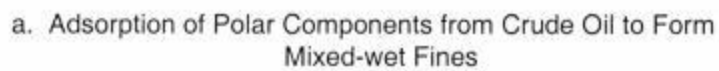
2.4 LOW SALINITY STUDIES

2.4.1 Mechanisms

There exist several mechanistic explanations for low salinity waterflood published by researchers but none of them has so far been generally accepted as the main mechanism.

Fines Migration

Tang and Morrow (1999a) conducted several corefloods on Berea sandstone cores and also on other reservoir. Some of the Berea cores were fired and acidized to remove the clay contents before use. The researchers reported no sensitivity of waterflood and imbibition behavior to decrease in salinity for these clay-free cores. Also when refined oil was used instead of crude oil, salinity had no effect on recovery. Lastly when cores were initially 100% saturated with crude oil, i.e., the fines were initially immersed in the oil phase, cores were insensitive to brine salinity. Tang and Morrow (1999a) concluded that the presence of clays, an initial water saturation and crude oil were all necessary conditions for low salinity waterflooding to increase oil recovery. Considering these factors, the authors proposed the following hypothesis: 1) heavy polar components of crude oil adhere to fine particles at pore walls and remain during displacement. 2) the mixed-wet clay particles detach from the pore walls by changing brine chemistry (Fig. 2-7). They further investigated the effect of low salinity brine on rock and other properties by numerous waterflooding tests (Tang and Morrow, 2002). They reported a reduction in brine permeability due to fines migration and confirmed that the presence of potentially mobile fines such as kaolinite played a key role in increased oil recovery.



16

Increase in pH

Since Morrow *et al.* progressed the research on the impact of brine salinity on oil recovery, researchers at BP began evaluating the applicability of low salinity waterflooding in the field scale. Webb *et al.* (2004) performed a log-inject-log field test in the Middle East to determine residual oil saturation to both high and low salinity waters. Three different brines (220,000 ppm, 170,000 ppm, and 3,000 ppm) were injected in the order into the reservoir from a producing well and results showed that injecting low salinity water significantly reduced remaining oil saturations in the near well bore region. McGuire *et al.* (2005) conducted four sets of single well chemical tracer tests in Alaska's North Slope reservoir. Residual oil saturation was substantially reduced by low salinity water injection in all cases, accompanied by an increase in effluent pH. The authors attributed the oil recovery increase to natural surfactant generation (saponification), which changed wettability and reduced interfacial tension (IFT).

Multi Ion Exchange (MIE)

BP researchers continued to study low salinity waterflooding and trademarked the process as LoSal[™] EOR Process. Lager *et al.* (2006) discussed the responsible mechanism for improved oil recovery by low salinity brine injection. They reported that multi-component ionic exchange between mineral surfaces and invading brine was the primary mechanism behind. The authors suggested that during aging, crude oil can be attracted or adsorbed to the surface through specific interactions (Fig. 2-8) and during a low salinity waterflood, it is possible the divalent cations are exchanged for monovalent cations which no longer hold the oil to the

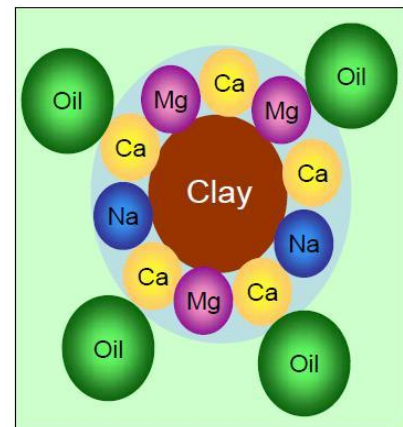


Figure 2-8: Schematic of Oil & Clay
(Lee *et al.* 2010)

surface. They also concluded that fines migration proposed by Morrow *et al.* and pH induced IFT reduction suggested by McGuire *et al.* may not always be present in low salinity waterflooding. Based on this assumption, Lager *et al.* (2007) suggested that kaolinite plays the most important role and proposed a correlation between kaolinite content and additional oil recovered by low salinity water.

Mineral Dissolution

Pu *et al.* (2008) proposed that the interstitial dolomite crystals play a role in low salinity recovery mechanisms. They injected coalbed methane (CBM) water into sandstone cores from the Tensleep formation in Wyoming which had very low clay content. Low salinity waterfloods were performed in tertiary mode. In all cases CBM water liberated additional oil except for the cores which was acidized and had no dolomite. Pu *et al.* suggested that some of dolomite clays became mixed-wet as they contacted the oil phase during aging and they might detach from the pore walls releasing oil from the rock surface during low salinity waterflood.

No Response

There are several publications indicating no benefit of low salinity waterflooding. Filoco and Sharma (1998) observed no improved oil recovery by reducing injection brine salinity but reported an increase in oil recovery only when the connate water salinity was reduced. These results indicated no benefit of low salinity waterflooding because connate water salinity cannot be manipulated in the field practice. Skrettingland *et al.* (2010) proved the deficiency of low salinity water in both laboratory measurements and a field test in the North Sea. They proposed that the initial wetting condition is a crucial property for the effect of low salinity waterflood and the wetting conditions in the North Sea field was naturally close to optimal such that sea water injection already was efficient.

2.4.2 Recent Work

There have been a growing number of publications related to low salinity waterflooding both in the laboratory scale and the field scale since SPE Symposium on Improved oil Recovery, Tulsa in 2006 (Fig. 2-9). Despite this growing interest in low salinity study, the mechanism behind the low saline EOR process is still uncertain. The complexity of the crude oil/brine/rock interactions and also variations in test procedures may contribute to confusion about the cause of low salinity effect. “The varieties of circumstance under which low salinity effect may or may not be observed suggest that more than one mechanism may be in play” (Morrow and Buckley, 2011).

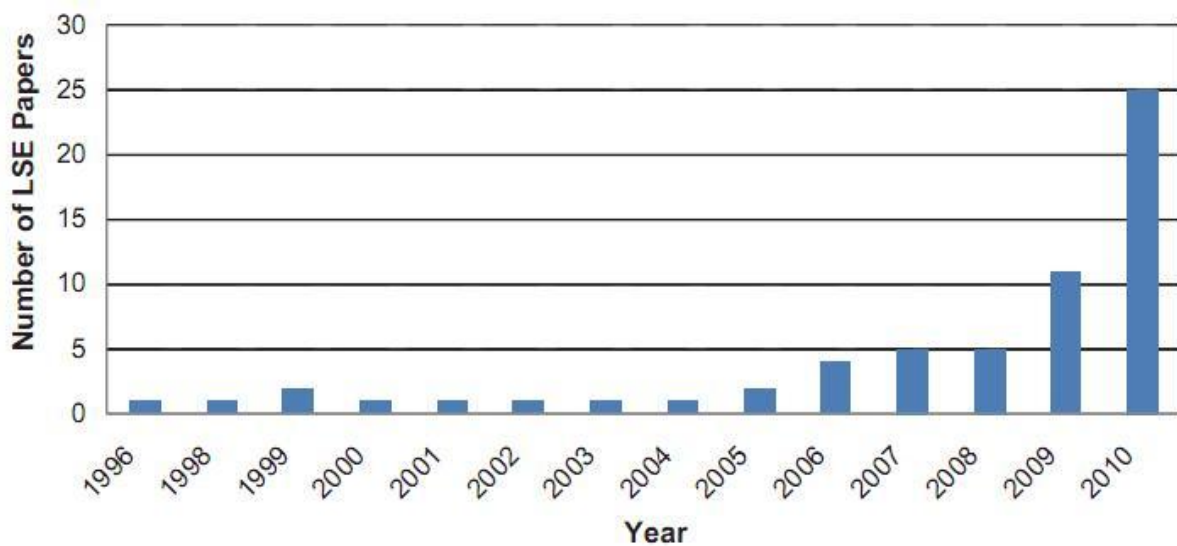


Figure 2-9: The Number of Publications and Presentations Focused on Low Salinity Waterflooding (Morrow and Buckley, 2011)

Necessary Conditions

Austad *et al.* (2010) listed the following conditions for low salinity effects by summarizing work done by Morrow's research group and researchers at BP.

Table 2-2: Conditions for Low Salinity Effects Listed by Austad *et al.* (2010)

Porous medium	-Clay must be present (kaolinite?)
Oil	-Must contain polar components (i.e. acids and bases)
Formation brine	-Formation water must contain divalent cations (i.e. Ca^{2+} , Mg^{2+}) -Initial water must be present. -Efficiency is related to initial water saturation S_{wi} .
Low salinity brine	-Salinity is usually between 1,000-2,000 ppm but effects have been observed up to 5,000 ppm. -Appears to be sensitive to ionic composition (Ca^{2+} vs. Na^{+})
Produced water	-pH of the effluent water usually increases about 1-3 pH units when injecting low salinity fluid. -In some cases, production of fines has been detected.
Permeability	-Usually an increase in pressure drop is detected during low salinity waterflood. -Sometimes there is no variation in end point relative permeability data between high and low salinity waterfloods.
Temperature	-There appears to be no temperature limitations to where low salinity effects can be observed.

Secondary Recovery vs. Tertiary Recovery

In a tertiary flooding, the core is first flooded with formation water until no more oil comes out and thereafter, the injected fluid is switched to low salinity water. When performing a secondary low salinity flood, the core is restored to native wettability at a low S_{wi} and a new waterflood is performed with the low saline water. In the literature, low salinity coreflood experiments showed a good success in both secondary and tertiary mode (Zhange *et al.* 2007; Agbalaka *et al.* 2009), but in some cases for only one or the other (Zhang and Morrow, 2006). Rivet *et al.* (2010) never observed incremental oil recovery in the tertiary mode. However, very often it is observed that the increase in oil recovery is higher in the secondary flood compared to the tertiary flood.

Reservoir Tests

In the past several years, a number of field trials have been conducted to evaluate the applicability of low salinity waterflooding in the field scale. Robertson (2007) showed some evidence of the beneficial impact of injection brines with well-selected ionic composition from historical field data. Larger *et al.* (2008) observed a significant increase in oil recovery after high salinity water injection and miscible injection, and a measurable drop in water-oil ratio (WOR) in an Alaskan reservoir. Recovery of residual oil between wells separated by 1,000 ft in Alaska was recently reported by Seccombe *et al.* (2010). More field studies showing positive response to injection of low salinity water have been published (Seccombe *et al.*, 2008; Batias *et al.*, 2009; RezaeiDoust *et al.*, 2010). However, a candidate North Sea field satisfying the necessary conditions for low salinity effect did not respond in either laboratory or pilot tests (Skrettingland *et al.*, 2010). This result may be discouraging to apply low salinity waterflooding, but it gives consistency between laboratory and field tests, which is encouraging to screen low salinity waterflood candidates.

Newly Proposed Mechanisms

Recently several researchers explained the wettability alteration process by low salinity in terms of double layer effects (Ligthelm *et al.*, 2009; Lee *et al.*, 2010). It was proposed that by lowering the overall salinity and especially multivalent cations in the brine solution, the electrical diffuse double layers between the clay and oil interfaces expands, which yields increased electrostatic repulsion (Fig. 2-10). Once the repulsive forces exceed the binding forces between clay and oil particles, the oil particles may be released from the rock surface and hence wettability changes towards water-wet.

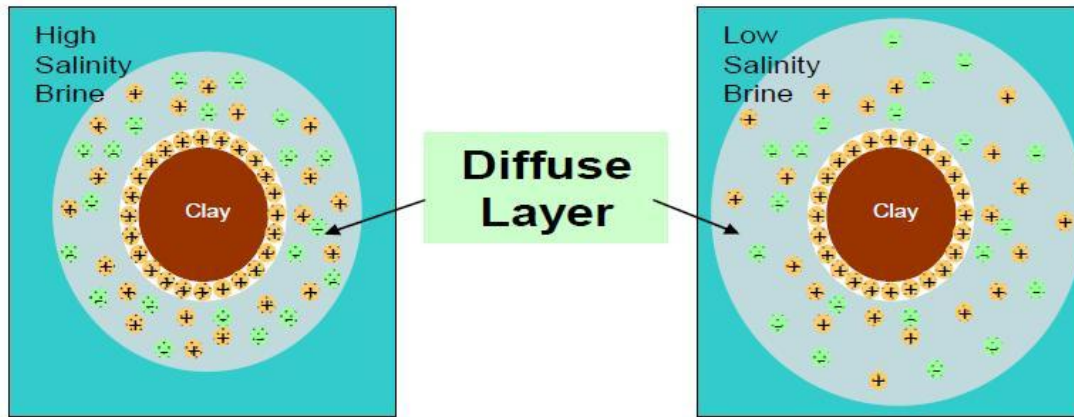
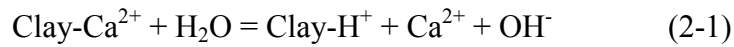


Figure 2-10: Impact of Salinity on Electrical Double Layer (Lee *et al.*, 2010)

RezaeiDoust *et al.* (2009) hypothesized a chemical mechanism termed “salting-in effects”. It was suggested that a decrease in salinity can increase the solubility of organic components in water (salting-in), which partially contributes to desorption of some organic materials loosely bonded to the clay surface. Researchers also attributed improved water wetness to the release of cations from the clay surface.

More recently, a chemical mechanism associated with local increase in pH was proposed by Austad *et al.* (2010). They suggested that injection of low salinity water disturbs the chemical equilibrium associated with brine-rock interaction and induces a net desorption of cations, especially Ca^{2+} . In order to compensate for the loss of cations, H^+ from the water near the clay surface adsorb onto the negatively charged clay. The substitution of Ca^{2+} by H^+ is illustrated by the following equation:



Researchers suggested this chemical reaction creates a local increase in pH close to the clay surface, which causes reactions between adsorbed basic and acidic material as in an ordinary acid-base proton transfer reaction (Fig. 2-11).

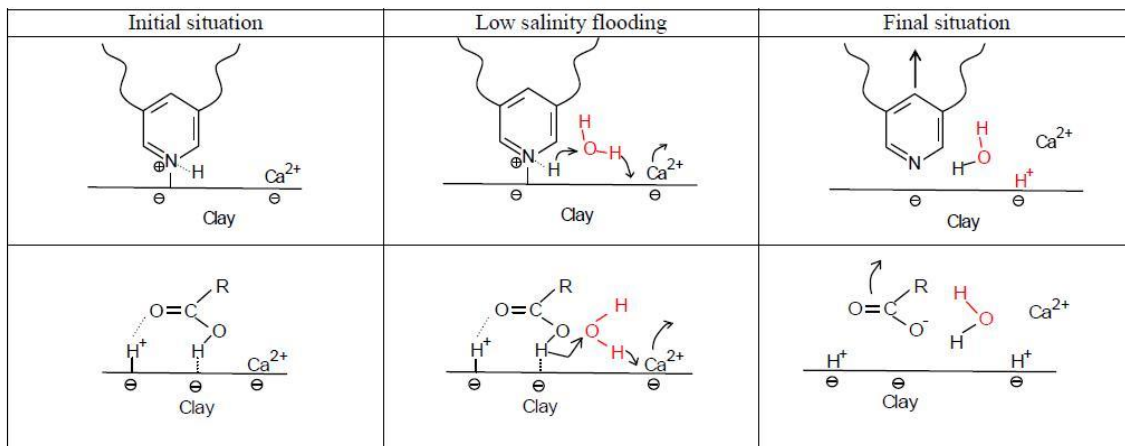


Figure 2-11: Proposed Mechanism for Low Salinity EOR Effects (Austad *et al.*, 2010)

2.5 COMBINED LOW SALINITY STUDIES

After a decade of extensive research on the low salinity effect, it is now generally agreed that oil recovery can be higher for low salinity brine injection compared to injection of seawater or high salinity brine. Based on the positive results from low salinity waterflooding, researchers began investigating combined low salinity flooding, such as low salinity surfactant flooding and low salinity polymer flooding.

Low salinity surfactant flooding is an economically attractive EOR process because using surfactant at low salinity conditions improves surfactant solubility and reduces adsorption or retention. Alagic and Skauge (2010) performed coreflood of combined low salinity water injection and surfactant flooding. All the low salinity surfactant (LS-S) floods were conducted in the tertiary mode. Significantly higher oil recovery was obtained for LS-S flood when the core was pre-flushed with low salinity brine compared to LS-S flood in high salinity environment. It was proposed that at low salinity, surfactant stayed in aqueous phase and microemulsion was successfully formed while surfactant moved over to oil phase and was trapped there at increased salinity conditions.

Polymer flooding is another promising way for low salinity water applications. When low salinity water is used in polymer mixing instead of seawater, considerably lower amount of polymer is required to achieve a target polymer solution viscosity. Figure 2-12 shows the effect of salinity on consumption of polymer, Flopaam 3630S in this case. Flopaam 3630S is the most widely used higher molecular weight polymer for EOR applications. Ayirala *et al.* (2010) conducted cost-performance analysis on offshore low salinity polymer flooding. It was concluded that low salinity polymer flooding was more cost-effective compared to seawater polymer flooding due to lower polymer consumptions and incremental oil recovery as a result of low salinity waterflooding

benefits. Authors also proposed that other EOR processes such as ASP flooding and steam floods might be also applicable to the low salinity system.

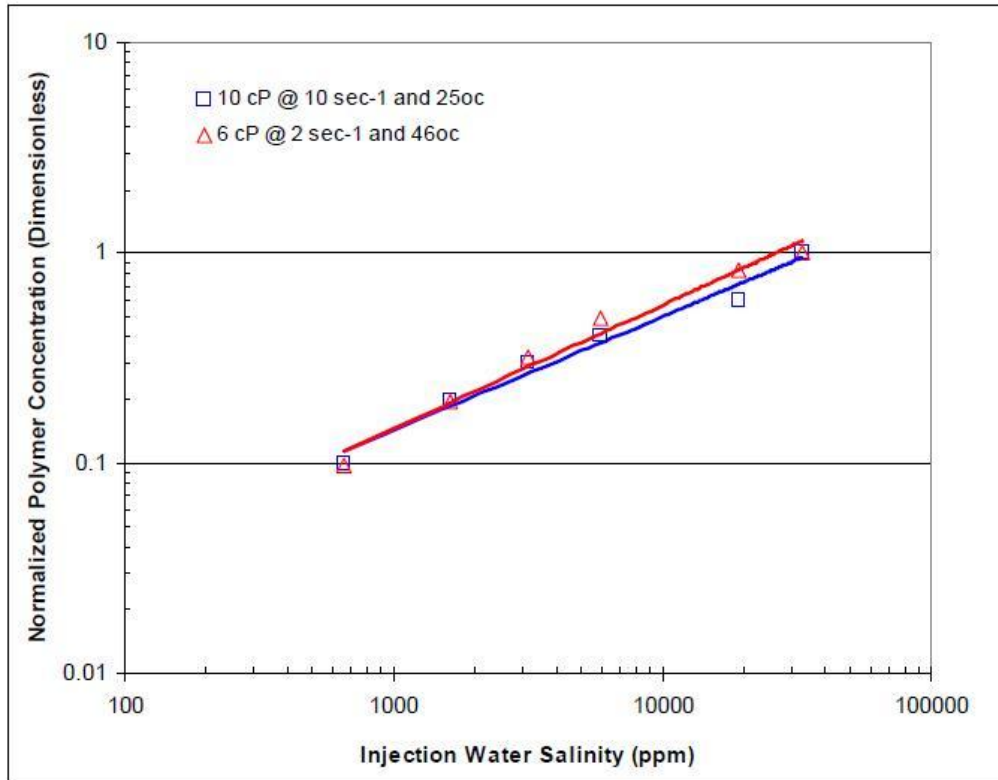


Figure 2-12: Effect of Salinity on Polymer Concentration (Ayirala *et al.*, 2010)

CHAPTER 3: MATERIALS, EQUIPMENTS, METHODOLOGY, AND DATA ANALYSIS

3.1 MATERIALS

3.1.1 Aqueous Phases

All the common salts such as NaCl and CaCl₂ were supplied by Fisher. Table 3-1 lists the components and corresponding composition of all the brines used in this study.

Table 3-1: Composition of Brines

Components	Synthetic Formation Brine (SFB)	Low Salinity Brine (LSB1)	Low Salinity Brine 2 (LSB2)
NaCl	28,620	1,000	2,862
KCl	650		65
CaCl ₂ -2H ₂ O	2,710		271
MgCl ₂ -6H ₂ O	3,890		389
TDS (ppm)	33,793	1,000	3,379

3.1.2 Polymers

The main objective for using polymer in chemical flooding is to provide enough viscosity to increase sweep efficiency and prevent fingering. Hydrolyzed polyacrylamides (HPAM) are common polymers for EOR application. HPAM is a polyelectrolyte with negative charges on the carboxylate groups with an average molecular weight of HPAM in the range of 1 to 20 million. In this study, medium molecular weight HPAM polymer, FlopaamTM 3330S was selected due to the low/moderate permeability of the Berea sandstone cores used.

3.1.3 Crude Oil

The crude oil obtained from Field A, referred to as Crude A, was used for all of the experiments. Crude A has a viscosity of 12 cp at 85°C (reservoir temperature). The crude oil was filtered through 0.45 µm cellulose filter before use.

3.1.4 Rocks

Berea sandstone core samples have been recognized by the petroleum industry as the best stone for testing the efficiency of chemical flood in the laboratory. Berea sandstone is a sedimentary rock whose grains are predominantly sand-sized and are composed of quartz sand held together by silica. 1-foot-long Berea sandstone cores with brine permeability in the range of 50 to 100 mD were used in all of the experiments. A representative core sample was evaluated for mineralogy and the result is listed below.

Table 3-2: Report of Rock Mineralogy Analysis (weight%)

Clays	Chlorite	1
	Kaolinite	2
	Illite	2
	Mx I/S*	0
Carbonates	Calcite	0.26
	Fe-Dol	2
	Siderite	1
Other Minerals	Quartz	86
	K-spar	4
	Plag.	2
	Pyrite	0.27
	Zeolite	0
	Barite	0
Totals	Clays	5
	Carb.	3
	Other	92

3.2 EXPERIMENTAL EQUIPMENTS

3.2.1 Coreflood Experimental Equipments

Glass Columns

The Kontes Chromaflex[®] columns were used to contain oil and a core sample for aging. These columns were 1 foot in length and 2 inches in outer diameter. The end pieces include a Vitron O ring and washer to prevent leaking when hand-tightened. The columns can withstand up to 50 psi.

Stainless Steel Accumulators

The Core Lab[®] stainless steel accumulators were used for fluid injection under high pressure. These accumulators were used in oil flood and polymer flood experiments involving high pressure. To inject fluid into the core, the column was oriented vertically and mineral oil from the pump was injected into the top, pushing the piston inside and then displacing the more dense fluid at the bottom. The piston material is Teflon, which prevents any galling from occurring between the piston and the honed cylinder wall.

Pumps

A Teledyne ISCO 5000 syringe pump was used to inject the fluid into the core at constant flow rate. Teledyne pumps use corrosion resistant stainless steel for cylinders and piston and heavy duty Teflon seals. In oil/polymer flood experiments, the pump was filled with mineral oil to displace the fluid in the accumulators into the core. In water flood experiments, the pump was filled with brine and fluid was directly injected to the core.

Core Holder

A stainless steel core holder manufactured by Phoenix Instruments was used. The core holder has 1.5” internal diameter and two pressure taps placed 20 cm apart from each other.

Pressure Transducers

The pressure drops for different sections across the core were measured by pressure transducers. Measured pressure drops by transducers are converted into output voltage and then read by a data acquisition recorder on the computer. The signals are then converted to a calibrated pressure for recording. Transducers should be calibrated prior to each experiment.

Data Acquisition Recorder

Signals from the pressure transducers were collected by National Instruments USB-6008 multifunction I/O board and transferred to the system named DATAQ Instruments Hardware Manager. Raw data were recorded as .DAT Microsoft Excel file with 1 second intervals

Fraction Collector

A Retriever[®] 500 Fraction Collector was used to collect effluent samples from water/polymer flooding. The collector can be programmed to collect the samples at fixed time intervals or fixed volume intervals.

Convection Ovens

Blue M[®] convection ovens are set to the temperature required during the experiments. Coreflood experiments were conducted in the oven to imitate the reservoir temperature. The oven was also used for aging. A digital display on the ovens indicates the real-time temperature.

Filter Presses

Solutions and oil were filtered by using a stainless steel OFITE filter press. Polymer solutions were filtered by a 1.2 μ m Millipore[™] hydrophilic cellulose filter paper. Oil and brine stocks were filtered through 0.45 μ m filter paper.

Figure 3-1 shows a schematic picture of coreflood setup including a core holder, accumulators, syringe pumps, pressure transducers and a convection oven. The core sample was placed in the core holder, which was located inside the oven to simulate reservoir temperature. Coil tubes were used to heat fluids ahead of the core face.

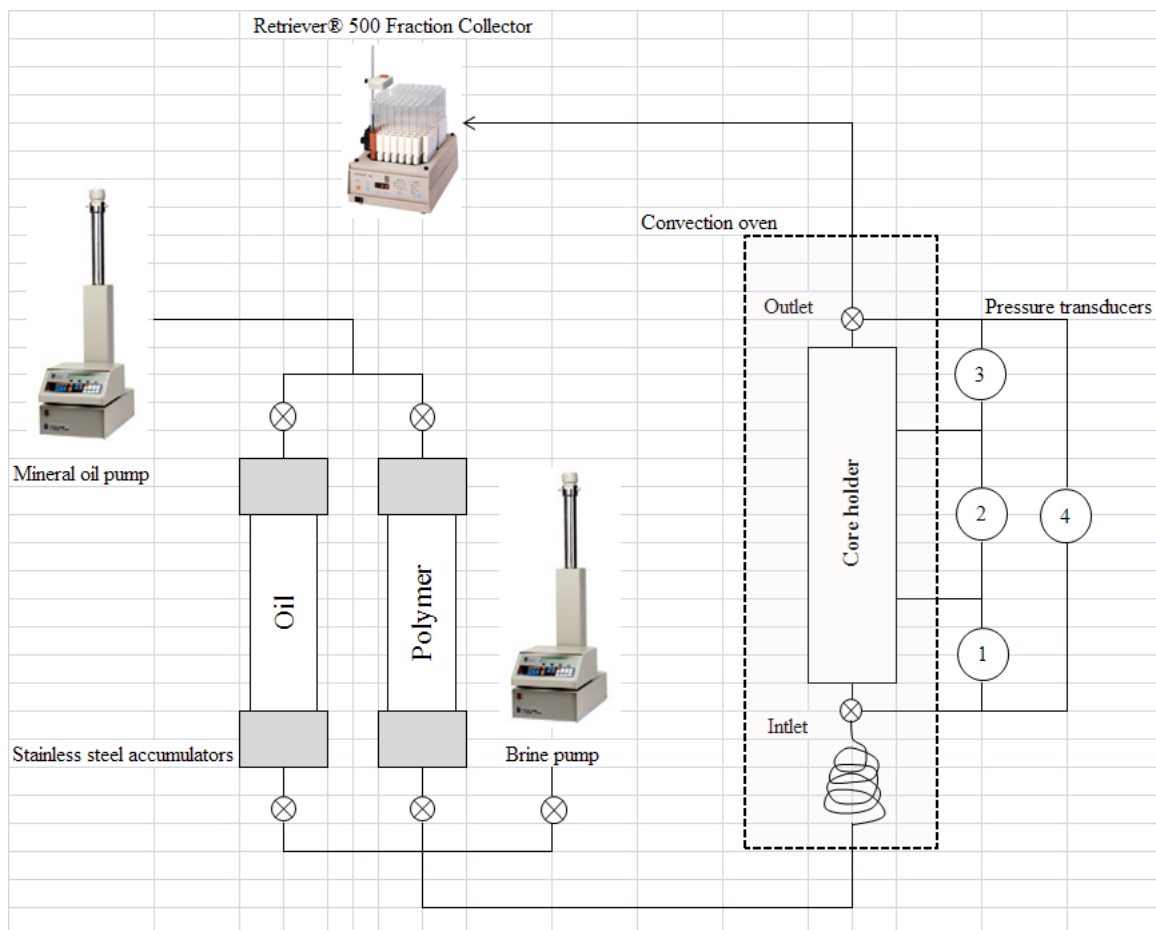


Figure 3-1: Schematic of Coreflood Setup

3.2.2 Analytical Equipments

pH Meter

pH was measured using a Fisher Science Education pH Meter. A pH probe was dipped into a sample to take a measurement. The sample was gently agitated until a steady reading was obtained.

Conductivity Meter

A Oacton CON 510 meter was used to measure conductivity of effluents samples. The meter's probe was submerged in a sample and an electric field was induced. The meter measured voltage drop between a current electrode and a pickup electrode, and calculated conductivity.

Rheometer

The bulk viscosity measurements were conducted using AR-G2 Rheometer from TA Instruments. The rheometer is suitable for inertia-free dynamic measurement of low viscosity fluids. It measures the torque generated by the sample in response to either an oscillatory or steady-shear strain deformation. Strain is applied by motor; torque is sensed by the transducer and converted to time-varying or steady properties whose results are displayed in the rheometer software named TA Orchestrator. The instrument requires the sample volume of 19 ml to operate properly.

Ion Chromatography

The cation concentrations in the effluents samples were directly measured by the Dionex ICS-3000 Ion Chromatography System. Before measurements, the effluent samples were filtered through a 0.2 μ m syringe filter for particle removal. Standard solutions were made to obtain calibration curves for each cations (Na⁺, K⁺, Ca²⁺, Mg²⁺, etc.)

3.3 METHODOLOGY

3.3.1 Fluid Preparation

Brine Stock

Deionized water and salts were mixed in the appropriate proportion. 1L of brine was mixed at a time. Every brine sample was filtered with the Millipore vacuum filter. Brine was poured into the filtration apparatus and a vacuum pump pulled the fluid through a 0.45µm cellulose filter.

Oil Stock

The oil sample was filtered with the OFITE filter press before use. Crude A was forced through a 0.45µm cellulose filter with applied air pressure of 20 psi at 85°C. Filtration procedure was done in a short time to prevent any evaporation of oil content. Viscosity of filtered Crude A at the reservoir temperature was measured by the rheometer.

Polymer Stock

Polymer solutions were prepared and diluted to the desired concentration. Polymer stocks were prepared by adding polymer powder to synthetic brine slowly and mixed for two days to avoid gel formation. After mixing, polymer solution was filtered through 1.2µm filter paper. Measured filtration ratio values using the following equation should be less than 1.2, indicating a homogeneous polymer stock solution.

$$\text{Filtration ratio} = \frac{\Delta t_{180} - \Delta t_{160}}{\Delta t_{40} - \Delta t_{20}} \quad (3.1)$$

Δt_x = time taken for collecting x ml of filtered polymer

Viscosity of filtered polymer solutions at the reservoir temperature was measured by the rheometer.

3.3.2 Core Preparation

All core samples used in this study were cut from the same block of Berea sandstone. All the core samples were 1.5 inch in diameter and approximately 1 foot in length. First the core was dried in the 100°C oven till it has constant weight. Then the core was wrapped by a heat shrink tape to prevent any damage. The core was then placed in the stainless steel core holder and 1,500 psi of confining pressure was applied using a mineral oil pump.

3.3.3 Coreflood Description

N₂/CO₂ Injection

After finishing core preparation and core assembly, compressed N₂ or CO₂ was injected into the core to determine gas permeability. N₂ or CO₂ was injected at several different constant pressure and flow rates were measured by a rotameter. Then gas permeability was calculated by a modified version of Darcy's law.

Brine Injection (at room temperature)

After gas permeability measurement, the core was flushed with synthetic formation brine. The objective of this brine injection was to determine absolute brine permeability. Several pore volumes of formation brine was injected at different constant flow rates (1-5 mL/min) until the pressure drop across the core was stable. Brine permeability at 100% brine saturation was calculated by Darcy's law.

Tracer Test

After brine permeability was determined, the core was flushed with tracer brine (normally lower-salinity brine than formation brine) at flow rate of 1-5 mL/min and effluent samples were collected by the fraction collector. The ion conductivity of the effluent samples was measured to determine the pore volume.

Brine Injection (at reservoir temperature)

After the pore volume was measured, experiment temperature was elevated to reservoir temperature, 85°C and the core was oriented vertically. Synthetic formation brine was again injected for several pore volumes to restore the connate water salinity in the core.

Oil Flooding (before aging)

After brine injection, prepared oil was injected into the core at high injection pressure at the reservoir temperature. The main purpose of oil flooding is to determine initial oil saturation, residual water saturation, effective oil permeability, and relative oil permeability. Oil flooding was conducted under a constant pressure (100-200 psi) to saturate the core with oil and to obtain accurate residual water saturation. 1.5~2.0 PV of oil was injected into the top end, considering density effect of oil and water. The effluent fluids were collected in 100 ml burettes and the volume of displaced water was measured to calculate residual water saturation and initial oil saturation. After water cut was less than 1% and pressure stabilized, oil was flooded at constant flow rate and the pressure drop across the core was recorded to calculate oil permeability.

Aging

After oil flooding, the core was taken out of the core holder and placed in a glass column filled with Crude A. The core was entirely immersed in oil and the column was sealed without leaking. The core was aged for 30~60 days at aging temperature, 90°C.

Oil Flooding (after aging)

After aging, the core was placed in the core holder again with confined pressure of 1,500 psi. Crude A was injected at a constant flow rate to flush out the oil inside the core. The pressure drop across the core was measured to calculate the oil permeability after aging.

Water Flooding

Water flooding with filtered brine was followed by oil flooding. Water flooding was conducted in order to determine residual oil saturation, effective water permeability, and relative water permeability after water flooding. Injection brines were synthetic formation brine for high salinity water flooding, and low salinity brine (<3,000 ppm) for low salinity water flooding. Low-rate water floodings were carried out at a typical reservoir advancement rate (~1 foot per day). The effluent fluids were collected in a burette and water flooding was stopped when oil cut was less than 1% and pressure was stabilized. The residual oil saturation was estimated based on the total volume of oil in burettes and effective oil permeability was calculated by the pressure drop across the core. Effluent fluids were analyzed by measuring pH and ion concentrations.

Polymer Flooding

Filtered polymer solution was injected after waterflooding in order to test performance of formulation and recover residual oil in the core as a tertiary recovery. Polymer flooding was conducted at a constant flow rate about 1-2 ft/day and the flooding was performed until no more oil was produced and the pressure was stabilized. pH, viscosity, and ion concentrations for the effluent fluids were analyzed to evaluate the performance of polymer flooding.

3.4 DATA ANALYSIS

Theoretical calculations and parameters used in core flood experiment are described below.

Pore Volume (Gravimetric)

The pore volume of core is calculated by mass balance. The gravimetric pore volume is equal to the difference in weight between dry core and saturated core divided by brine density.

$$V_p = \frac{m_{sat} - m_{dry}}{\rho_w} \quad (3.2)$$

V_p = pore volume

m_{sat} = mass of brine saturated core

m_{dry} = mass of dried core

ρ_w = brine density

Pore Volume (Tracer)

The pore volume can be also determined by tracer test. The pore volume is equal to the breakthrough of the injected conductivity. Conductivity is normalized to the initial and injected conductivity:

$$C_D = \frac{C - C_{int}}{C_{inj} - C_{int}} \quad (3.3)$$

C_{int} = conductivity of fluid

C_{inj} = conductivity of injected fluid

C_D = normalized conductivity

Normalized conductivity is plotted vs. volume injected and the area above the curve is integrated to determine the breakthrough and then pore volume.

Bulk Volume

The bulk volume of core is calculated by total volume of the bare core.

$$V_b = \pi r^2 L \quad (3.4)$$

V_b = bulk volume

r = radius of core

L = length of core

Porosity

The porosity of the core is pore volume divided by bulk volume.

$$\phi = \frac{V_p}{V_b} = \frac{V_b - V_s}{V_b} \quad (3.5)$$

Brine Permeability

The brine permeability, or absolute permeability is calculated based on Darcy's single phase, steady-state, and horizontal flow equation:

$$q = \frac{kA\Delta P}{\mu L} \quad (3.6)$$

q = flow rate

ΔP = pressure drop across core

k = absolute permeability

A = crosssectional area of core

μ = viscosity of fluid

Gas Permeability

Nitrogen/CO₂ Permeability is calculated by modified version of Darcy's law:

$$k_g = \frac{2q_{sc}\mu L P_{sc}}{A(P_1^2 - P_2^2)} \quad (3.7)$$

k_g = gas permeability

P_1 = pressure at inlet

P_2 = pressure at outlet

q_{sc} = flow rate at standard condition

P_{sc} = pressure at standard condition

Effective Oil/Water Permeability

Permeability to each flowing phase in the presence of another fluid is defined as effective permeability to that phase and calculated as:

$$k_{eff,j} = \frac{\mu_j q_j L}{A \Delta P_j} \quad (3.8)$$

$k_{eff,j}$ = effective permeability to phase j

μ_j = viscosity of phase j

q_j = flow rate of phase j fluid

P_j = pressure drop during phase j fluid injectio

End Point Relative Oil/Water Permeability

End Point relative permeability is calculated by dividing effective permeability by brine permeability.

$$k_{rj} = \frac{k_{eff,j}}{k} \quad (3.9)$$

k_{rj} = relative permeability to phase j

Initial Oil Saturation

An oil flood was conducted in the brine saturated core until residual water saturation was reached. Initial oil saturation was determined by mass balance: the volume of produced water is the volume of oil in the core. Thus initial oil saturation was estimated by dividing the volume of produced water by the pore volume as follows:

$$S_{oi} = \frac{V_w}{V_p} \quad (3.10)$$

S_{oi} = initial oil saturation

V_w = volume of water produced from oil flood

Residual Oil Saturation

The residual oil saturation from water flood was calculated after the oil cut was less than 1%. The volume of oil produced during water flood was the mobile oil saturation. Residual oil saturation was estimated by the following equation:

$$S_{orw} = \frac{V_w - V_o}{V_p} \quad (3.11)$$

S_{orw} = residual oil saturation after water flood

V_o = volume of oil produced from water flood

The residual oil saturation after polymer flood is the difference between the volume of oil remaining in the core after water flood and the volume of oil produced after polymer flood.

$$S_{orc} = \frac{S_{orw}V_p - V'_o}{V_p} \quad (3.12)$$

S_{orc} = residual oil saturation after chemical flood

V'_o = volume of oil produced from chemical flood

Oil Recovery

Oil recovery can be estimated after waterflood/polymer flood. Oil recovery was calculated by dividing the sum of oil recovered from core flood by the volume of oil initially saturated the core.

$$f_{op} = \frac{\sum_{i=1} V_{opi}}{V_{oi}} \quad (3.13)$$

f_{op} = fraction of oil produced

V_{opi} = volume of free oil collected in tube i

V_{oi} = initial volume of oil before waterflood

CHAPTER 4: RESULTS AND DISCUSSION

4.1 LOW SALINITY WATER FLOODING

In this experiment, a sequence of two high salinity secondary and two low salinity secondary waterfloods were conducted in a single Berea sandstone core (Berea A). The objective of this experiment was to evaluate the effect of low salinity water injection and aging time on residual oil saturation and relative permeability in the sandstone core. Water floodings were performed in the same core to eliminate the possibility of natural variation between cores.

A single core was cut from a block of visually homogeneous Berea sandstone. Two types of brine were used during waterflood experiments. A synthetic formation brine (SFB) with 33,793 ppm TDS was chosen for high salinity water and a low salinity brine (LSB) with 1,000 ppm for low salinity water. Properties of the core and fluids are given in Table 4-1 and 4-2 respectively.

Table 4-1: Berea A Core Properties

Length	(inch)	11.73
Diameter	(inch)	1.50
Bulk Volume	(ml)	339.67
Pore Volume	(ml)	61.81
Porosity	(%)	18.20
Nitrogen Permeability	(md)	137.52
Brine Permeability	(md)	83.03
Clay Content	(weight%)	5.00

Table 4-2: Experiment 4.1 Fluid Properties at 85°C and 10s⁻¹

Synthetic Formation Brine (SFB)	Concentration	(ppm)	28,620	NaCl
			650	KCl
			2,710	CaCl ₂
			3,890	MgCl ₂ ·6H ₂ O
			33,793	TDS
	Viscosity	(cP)	0.47	
Low Salinity Brine (LSB)	Concentration	(ppm)	1,000	NaCl
			1,000	TDS
	Viscosity	(cP)	0.47	
Crude Oil (Crude A)	Viscosity	(cP)	12	

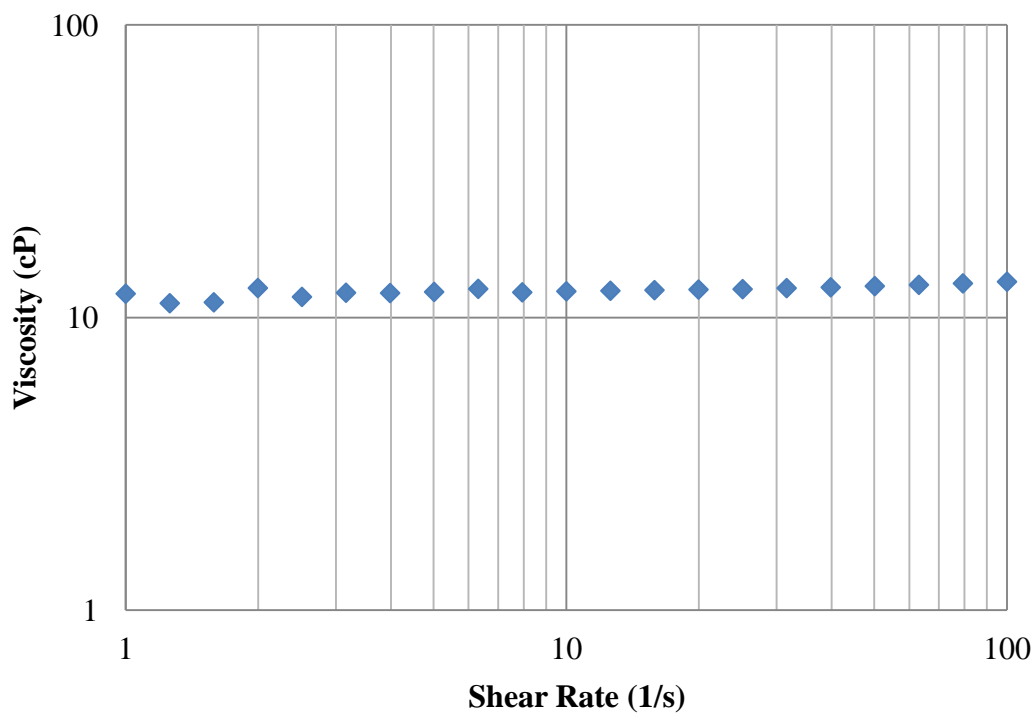


Figure 4-1: Crude A Viscosity vs. Shear Rate (T = 85°C)

After the initial core preparation (described in Chapter 3), the following floods were conducted: six oil floods (Oil Flood 1-6), four water floods (High & Low Salinity Waterflood 1-2), and three tracer tests (Tracer Test 1-3). Figure 4-2 shows a flow chart of the experimental procedure.

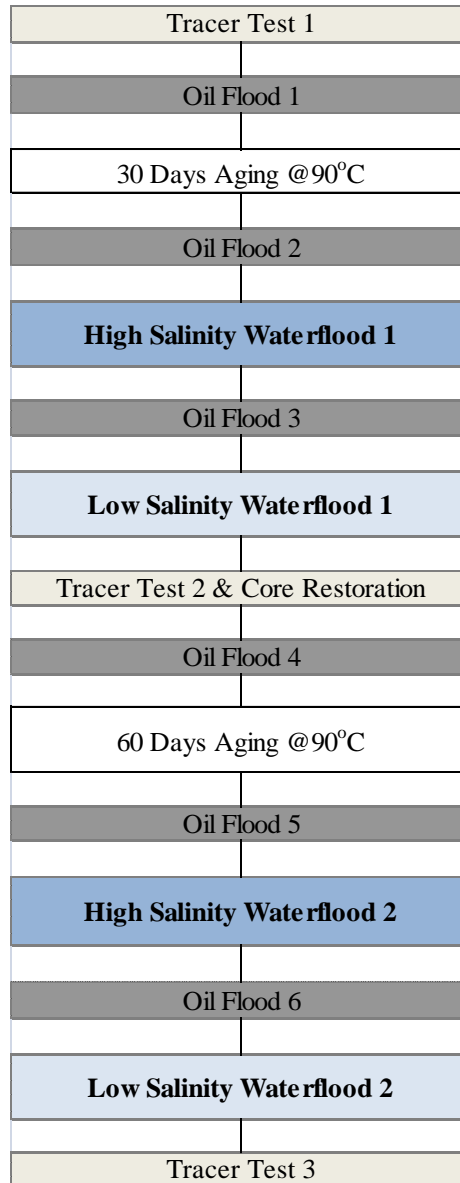


Figure 4-2: Experiment 4.1

Tracer Test 1

Tracer Test 1 was conducted at a flow rate of 5.0 mL/min to determine the pore volume of Berea A. Effluent samples were collected every 2 minutes with sample size of 10 mL. The measured conductivity was normalized on a scale of zero to one and plotted against the injected volume (Fig. 4-3). The calculated pore volume was 61.81 mL.

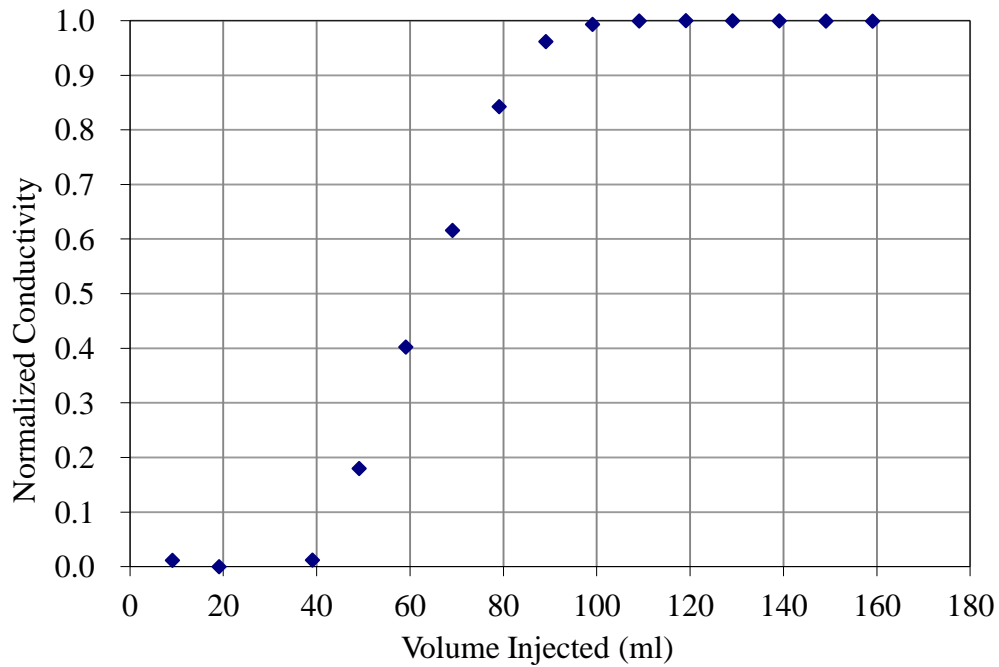


Figure 4-3: Effluent Conductivity History (Tracer Test 1)

Oil Flood 1

Oil Flood 1 was performed using Crude A at 85°C. The oil flood was performed at a constant inlet pressure of 200 psi. Once the oil flow rate reached steady state, end point oil relative permeability k_{ro}^o was calculated to be 0.57. The value of S_{oi} was determined by mass balance and came out to be 78.0 %.

30 Days Aging

After Oil Flood 1, the core was taken out of the core holder and placed in a glass column filled with Crude A. The core was entirely immersed in oil and the column was sealed without leaking. The core was aged for 30 days at aging temperature, 90°C. After aging, we put drops of brine on the surface of the rock to see its wettability. Drops remained on the surface without being absorbed and its contact angle was more than 90° (Fig. 4-4). This indicated that the Berea core A became mixed-wet.

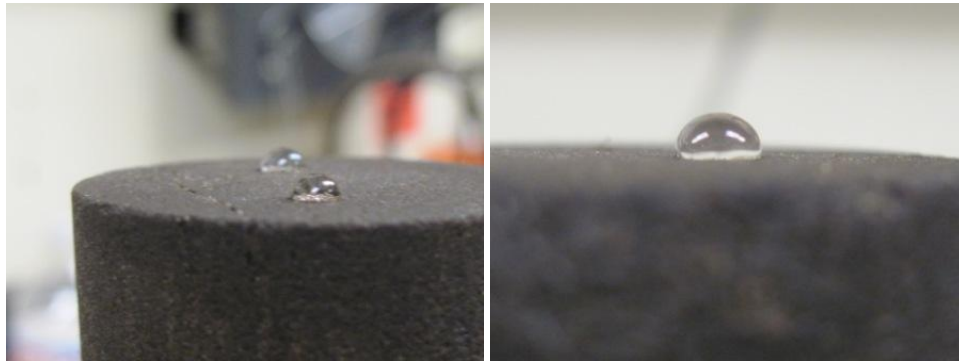


Figure 4-4: Brine Drops on the Surface of Berea A

Oil Flood 2

After aging, Berea A was flooded with Crude A at a flow rate of 0.5 ml/min for 2PV to flush out the oil inside the core. No water was produced during the flood. Once the pressure drop across the core reached steady state, k_{ro}^o was calculated to be 0.45. This oil permeability reduction also indicated wettability alteration toward oil-wet.

High Salinity Waterflood 1

A secondary waterflood using SFB was performed following Oil Flood 2. SFB was injected at a flow rate of 0.1 mL/min (2.28 ft/Day) for 4.6 PV. The pressure drop across the core was monitored during the flood (Fig. 4-5) and the final pressure drop was used to calculate end point water relative permeability k_{rw}^o once steady state was reached. Based on the final steady state pressure drop, $k_{eff,w}$ and k_{rw}^o were found to be 2.18 mD and 0.026 respectively. Figure 4-6 shows oil recovery, oil cut and average oil saturation from the waterflood. Water breakthrough occurred early at 0.15PV. Oil production stopped after around 2PV of water injection and final oil recovery was 50.3%OOIP. The residual oil saturation S_{or} was determined by mass balance and came out to be 38.7%.

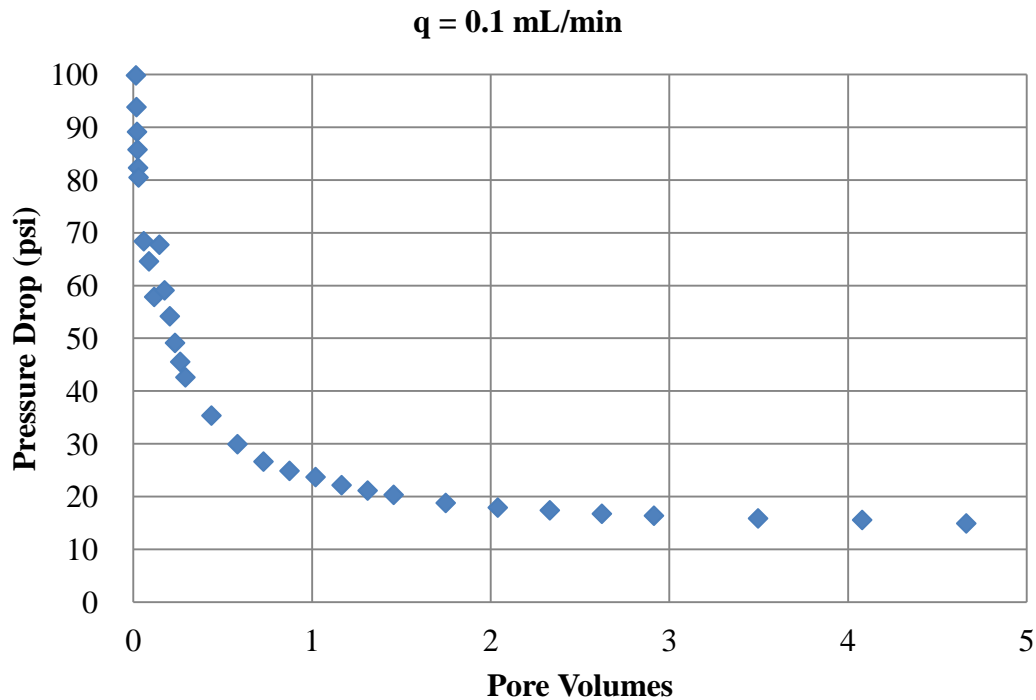


Figure 4-5: High Salinity Waterflood-1 Pressure Drop

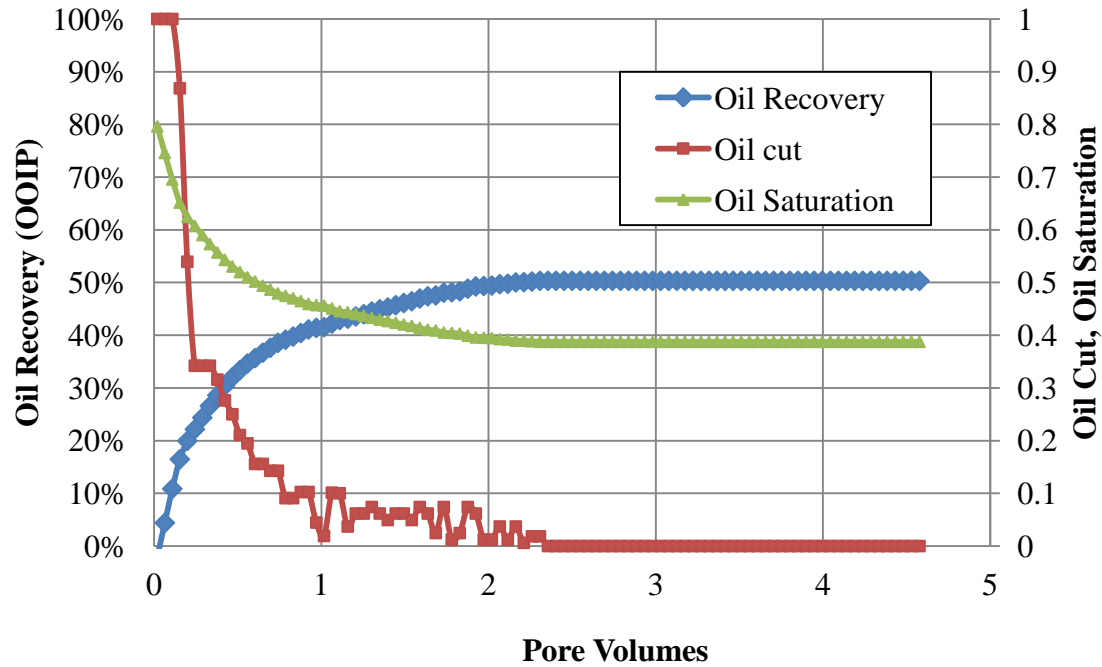


Figure 4-6: High Salinity Waterflood-1 Oil Recovery

Oil Flood 3

After High Salinity Waterflood 1, Crude A was injected at a rate of 0.5 mL/min to establish S_{oi} . Once the pressure drop across the core reached steady state, k_{ro}^o was calculated to be 0.48. The value of S_{oi} was determined by mass balance and came out to be 74.0 %.

Low Salinity Waterflood 1

A secondary waterflood using LSB was performed following Oil Flood 3. LSB was injected at a flow rate of 0.1 mL/min (2.28 ft/Day) for 9.4PV. The pressure drop across the core was monitored during the flood (Fig. 4-7) and the final pressure drop was used to calculate k_{rw}^o . Based on the final steady state pressure drop, $k_{eff,w}$ and k_{rw}^o were

found to be 1.05 mD and 0.013, respectively. There was significant permeability reduction compared to High Salinity Waterflood 1 and this can be explained by clay migration due to injection of very low salinity water with 1,000 ppm TDS.

Figure 4-8 shows oil recovery, oil cut and average oil saturation from the waterflood. Water breakthrough occurred at 0.24PV. Oil production stopped after around 2.5PV of water injection and final oil recovery was 53.2%OOIP. No clay particle was visually observed in effluent samples. The residual oil saturation S_{or} was determined by mass balance and came out to be 34.7%, which was 4% lower than that of High Salinity Waterflood 1.

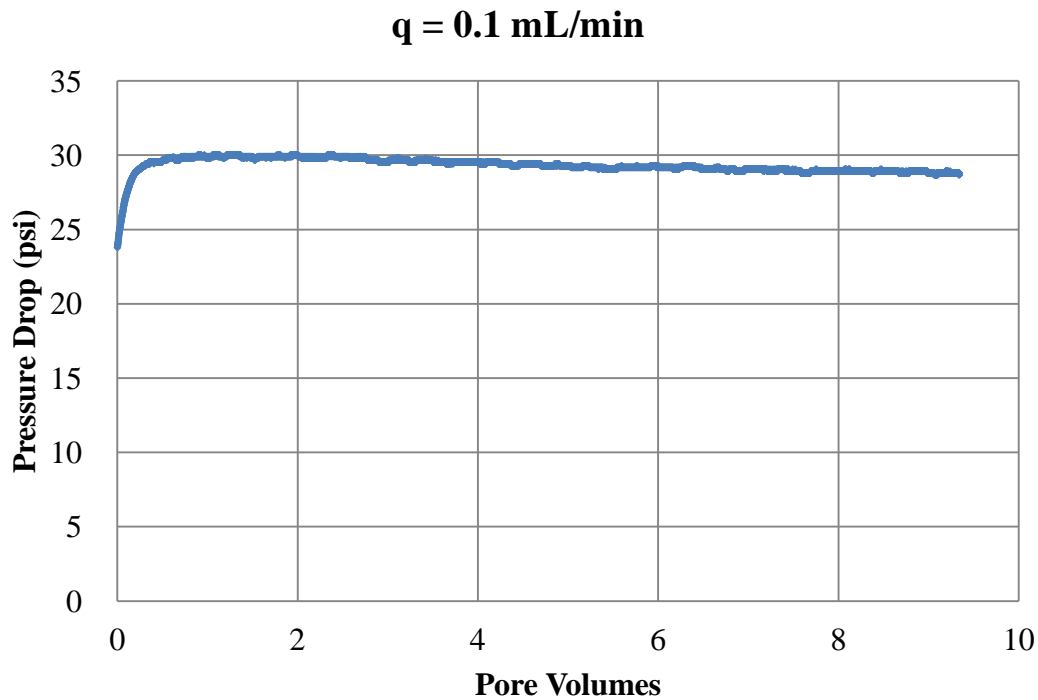


Figure 4-7: Low Salinity Waterflood-1 Pressure Drop

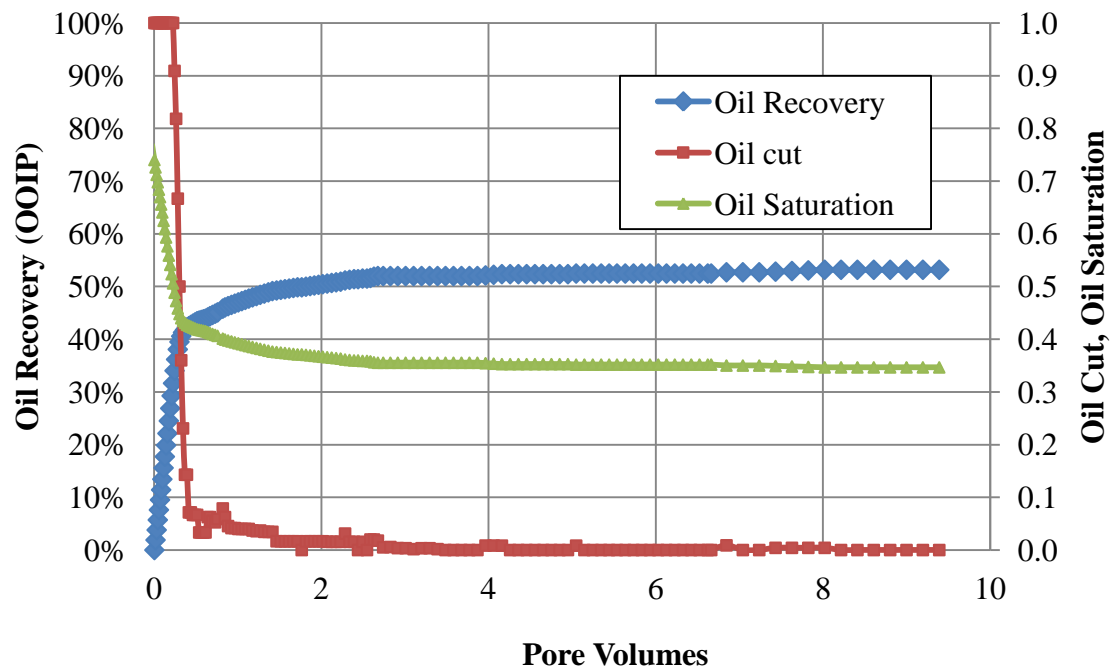


Figure 4-8: Low Salinity Waterflood-1 Oil Recovery

Tracer Test 2

SFB was injected at a flow rate of 0.1 mL/min for Tracer Test 2 to confirm the residual oil saturation and also to restore the core. No additional oil was recovered during the flood. Pressure drop across the core was monitored and is shown in Figure 4-9. According to the pressure data, permeability to water increased again to almost the same value obtained during High Salinity Waterflood-1. This might indicate that the permeability damage due to clay migration was reversible. Figure 4-10 illustrates effluent conductivity history from Tracer Test 2.

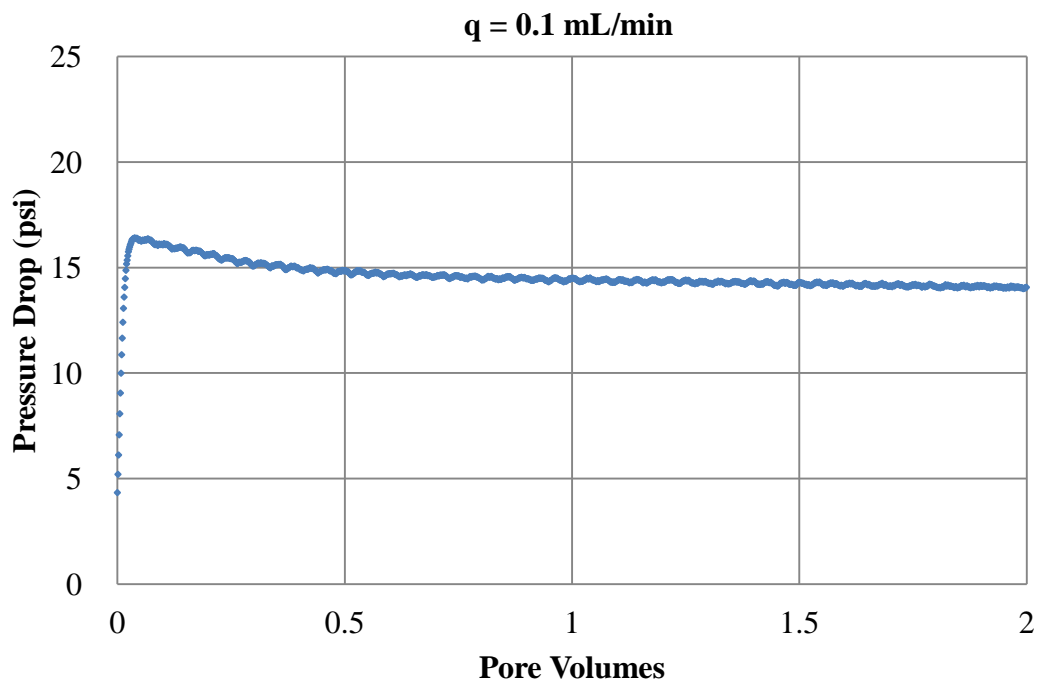


Figure 4-9: Tracer Test-2 Pressure Drop

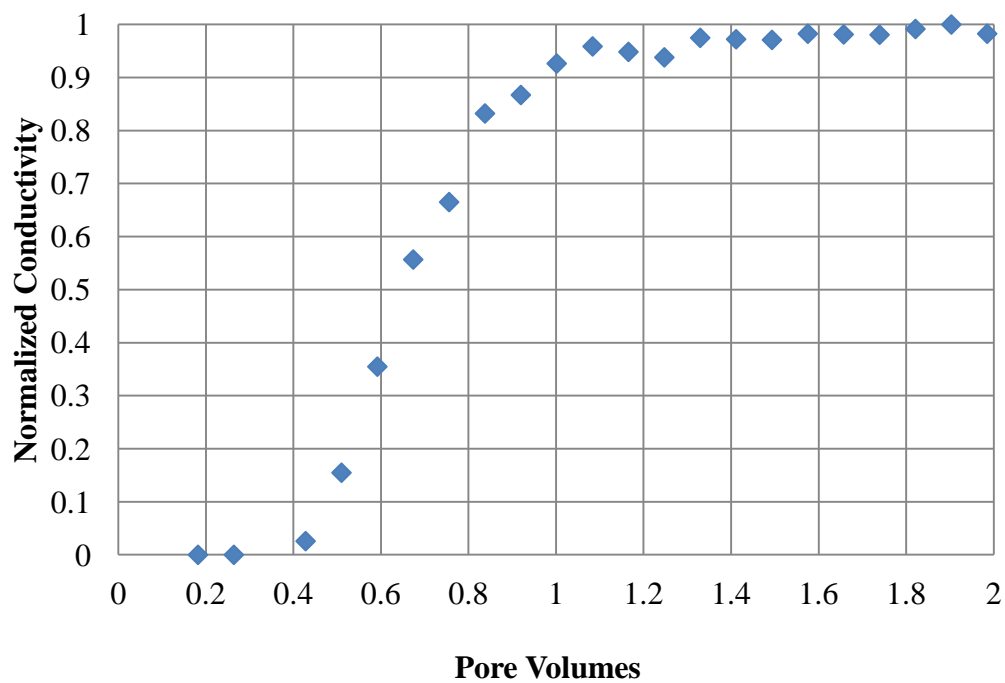


Figure 4-10: Effluent Conductivity History (Tracer Test 2)

Oil Flood 4

After Low Salinity Waterflood 2, Crude A was injected at a rate of 0.5 mL/min to establish S_{oi} . Once the pressure drop across the core reached steady state, k_{ro}^o was calculated to be 0.54. The value of S_{oi} was determined by mass balance and came out to be 81.0 %.

60 Days Aging

After Oil Flood 4, the core was re-aged for 60 days at aging temperature, 90°C.

Oil Flood 5

After aging, Berea A was flooded with Crude A at a flow rate of 0.5 ml/min for 2PV to flush out the oil inside the core. No water was produced during the flood. Once the pressure drop across the core reached steady state, k_{ro}^o was calculated to be 0.36, which was much lower than that before aging. This oil permeability reduction indicated that the core became more strongly oil-wet than the previously aged core.

High Salinity Waterflood 2

A secondary waterflood using SFB was performed following Oil Flood 5. SFB was injected at a flow rate of 0.1 mL/min (2.28 ft/Day) for 7.5PV. The pressure drop across the core was monitored during the flood (Fig. 4-11) and the final pressure drop was used to calculate end point water relative permeability k_{rw}^o once steady state was reached. Based on the final steady state pressure drop, $k_{eff,w}$ and k_{rw}^o were found to be 1.66 mD and 0.020 respectively.

Figure 4-12 shows oil recovery, oil cut and average oil saturation from the waterflood. Water breakthrough occurred early at 0.11PV. Oil production stopped after

around 2PV of water injection. Final oil recovery was 45.2%OOIP and it was 5% lower than recovery from the first high salinity waterflood. This may indicate that after 60-day-aging, the core became more oil-wet than the core aged for 30 days. Another possible explanation for the different behavior of the core is that Low Salinity Waterflood 1 somewhat changed core properties, which resulted in less oil recovery.

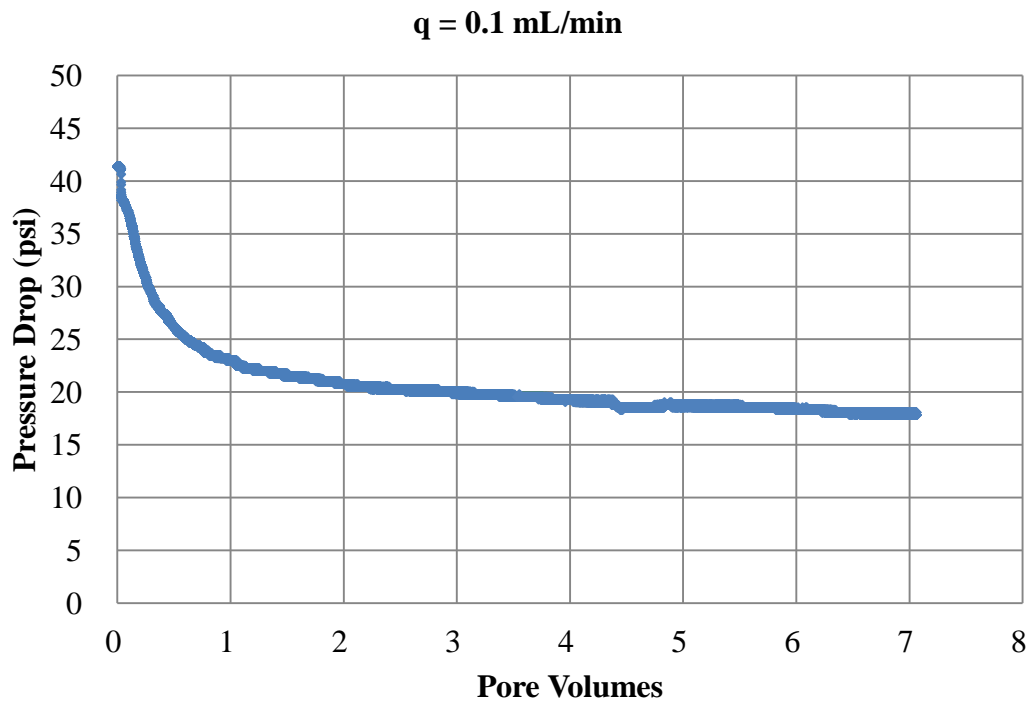


Figure 4-11: High Salinity Waterflood-2 Pressure Drop

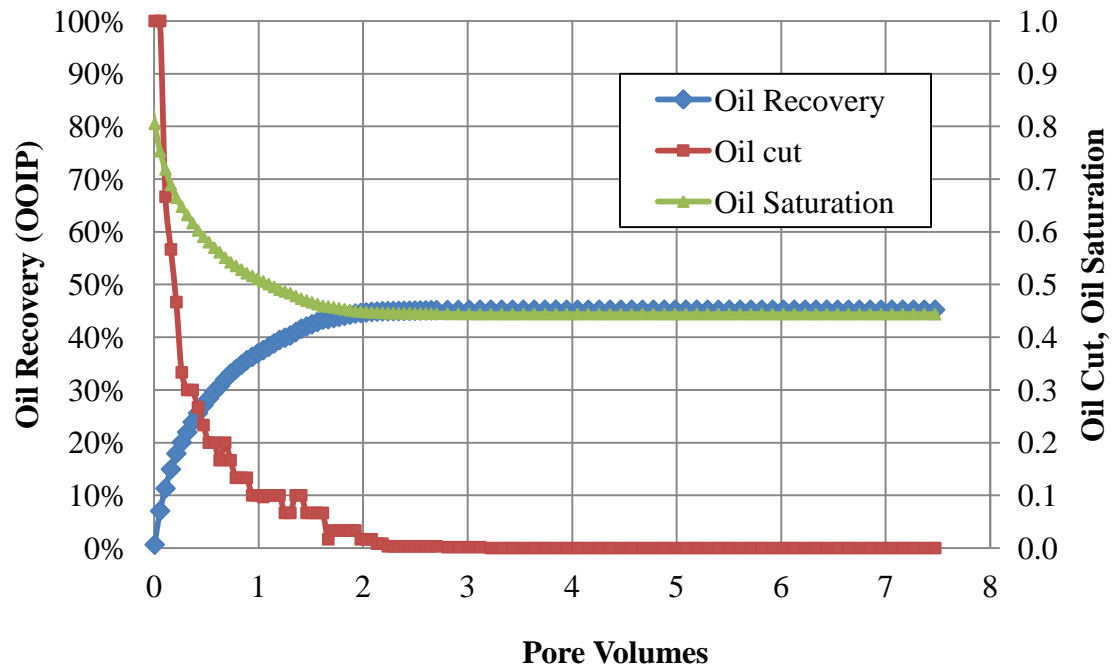


Figure 4-12: High Salinity Waterflood-2 Oil Recovery

Oil Flood 6

After High Salinity Waterflood 2, Crude A was injected at a rate of 0.5 mL/min to establish S_{oi} . Once the pressure drop across the core reached steady state, k_{ro}^o was calculated to be 0.34. The value of S_{oi} was determined by mass balance and came out to be 79.0 %.

Low Salinity Waterflood 2

A secondary waterflood using LSB was performed following Oil Flood 6. LSB was injected at a flow rate of 0.1 mL/min (2.28 ft/Day) for 5.5PV. The pressure drop across the core was monitored during the flood (Fig. 4-13) and the final pressure drop was used to calculate k_{rw}^o . Based on the final steady state pressure drop, $k_{eff,w}$ and k_{rw}^o

were found to be 1.68 mD and 0.020 respectively. There was no permeability reduction compared to High Salinity Waterflood 2. This may indicate that clay particle became less sensitive to brine salinity after a series of waterflooding.

Figure 4-14 shows oil recovery, oil cut and average oil saturation from the waterflood. Water breakthrough occurred early at 0.12PV. Oil production stopped after around 2.5PV of water injection and final oil recovery was 49.7%OOIP. No clay particle was visually observed in effluent samples. The residual oil saturation S_{or} was determined by mass balance and came out to be 39.7%. There was still an increase in oil recovery compared to the second high salinity waterflood.

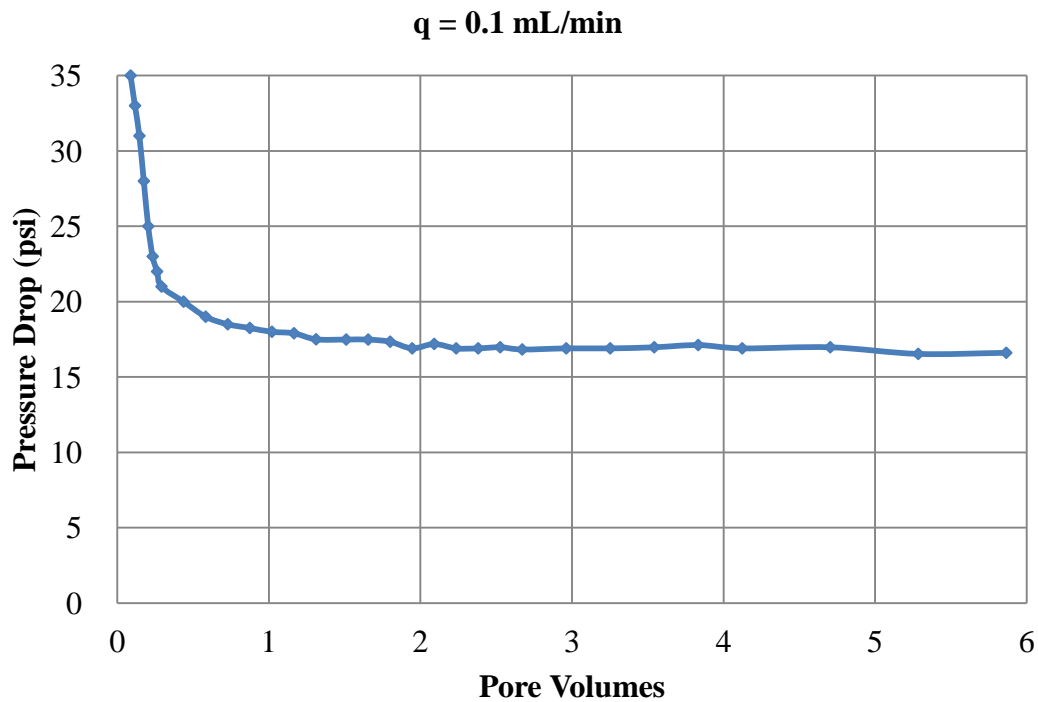


Figure 4-13: Low Salinity Waterflood-2 Pressure Drop

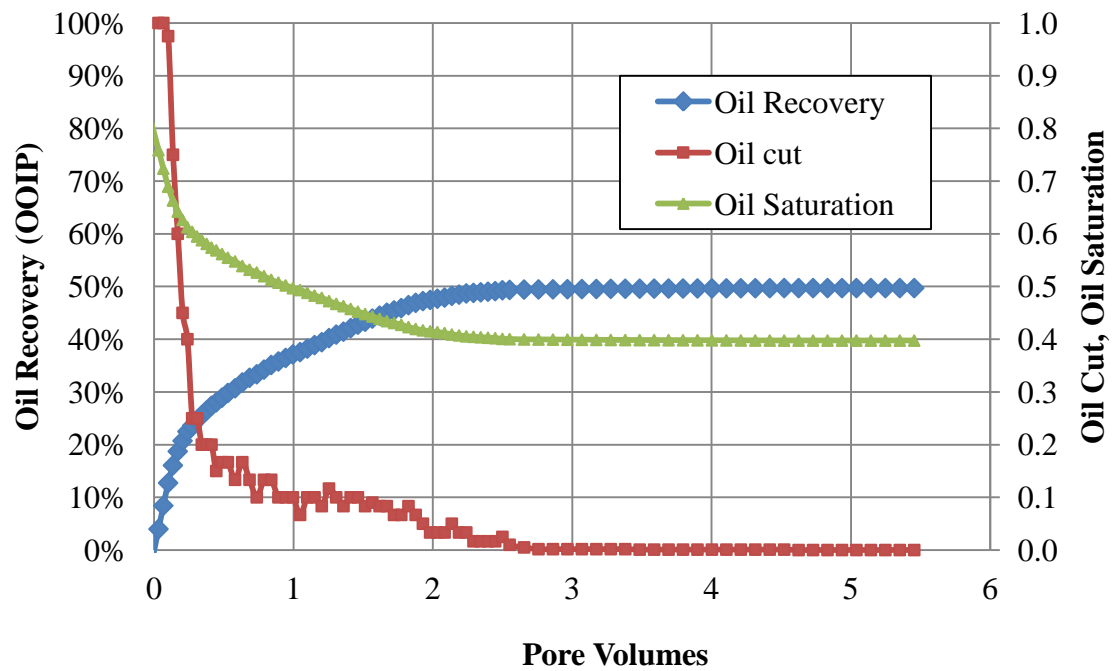


Figure 4-14: Low Salinity Waterflood-2 Oil Recovery

Tracer Test 3

SFB was injected at a flow rate of 0.1 mL/min to confirm the residual oil saturation. No additional oil was recovered during the flood. Figure 4-15 illustrates effluent conductivity history from Tracer Test 3.

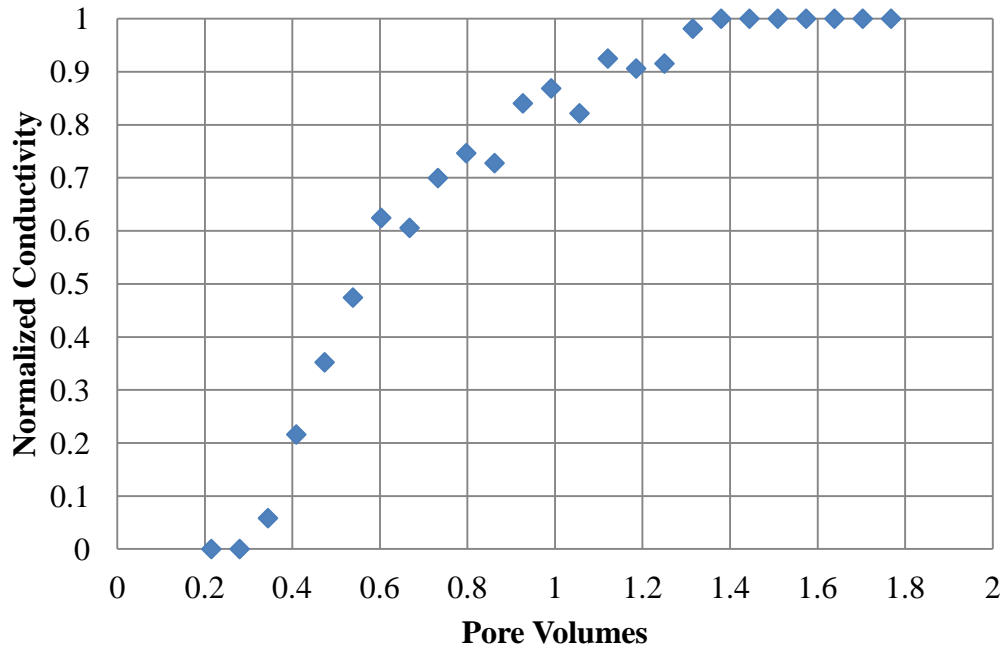


Figure 4-15: Effluent Conductivity History (Tracer Test 3)

Ion Concentrations

Effluent samples from waterfloods were analyzed using ICS-3000 system to measure concentrations of Na^+ , K^+ , Ca^{2+} , and Mg^{2+} cations. Figure 4-16 – 19 show ion concentrations versus pore volumes of water injected for each waterflood. In High Salinity Waterflood 1 and 2, ion concentrations are almost constant because concentrations of initial water and injected water were identical. In Low Salinity Waterflood 1 and 2, a sharp decline in all the ion concentrations was observed until 2 PV due to dilution of formation brine by low salinity brine. After 2 PV, Ca^{2+} and Mg^{2+} showed a constant increase while K^+ displayed a slight decrease. Ion concentrations of K^+ , Ca^{2+} , and Mg^{2+} did not reach zero during the flood even though injected brine had zero concentrations of these ions.

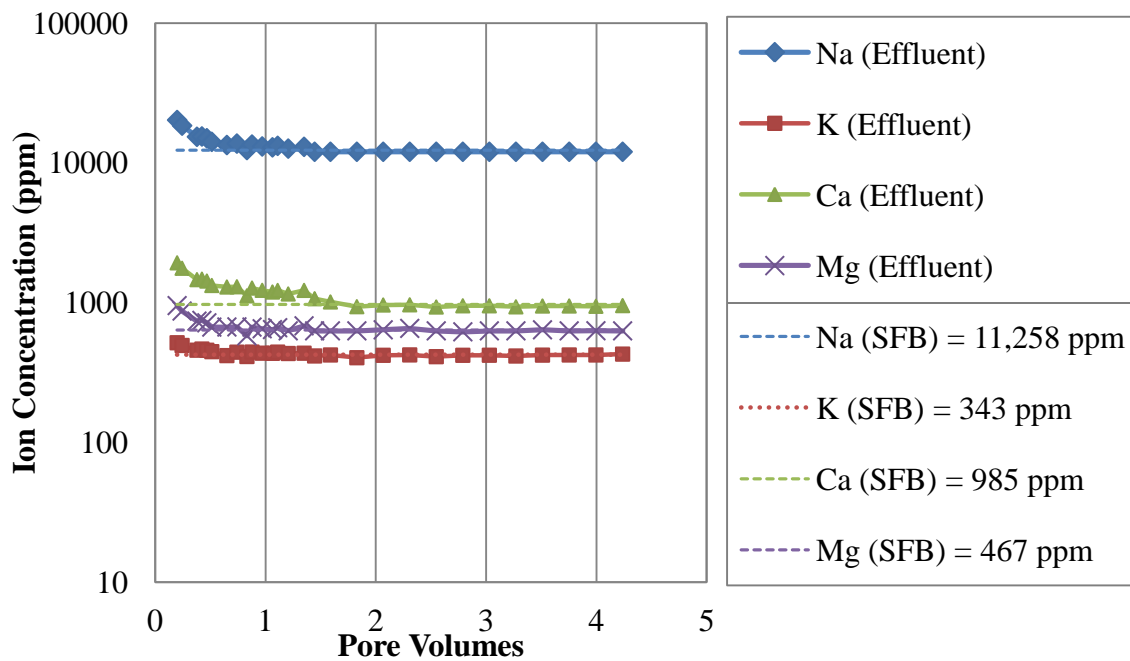


Figure 4-16: Effluent Ion Concentration of High Salinity Waterflood 1

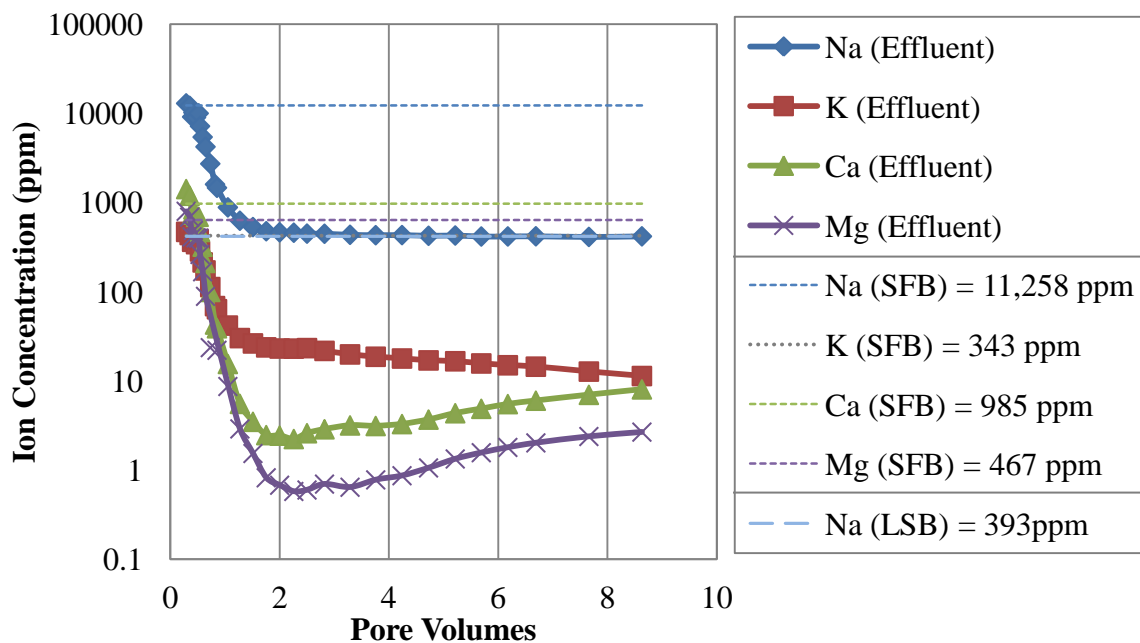


Figure 4-17: Effluent Ion Concentration of Low Salinity Waterflood 1

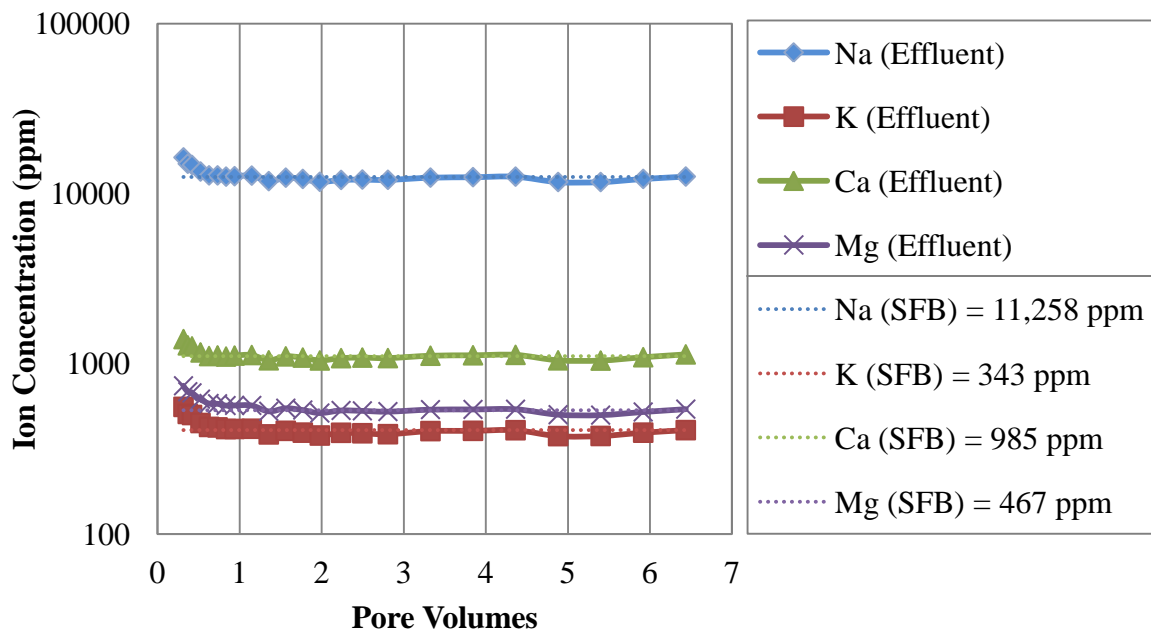


Figure 4-18: Effluent Ion Concentration of High Salinity Waterflood 2

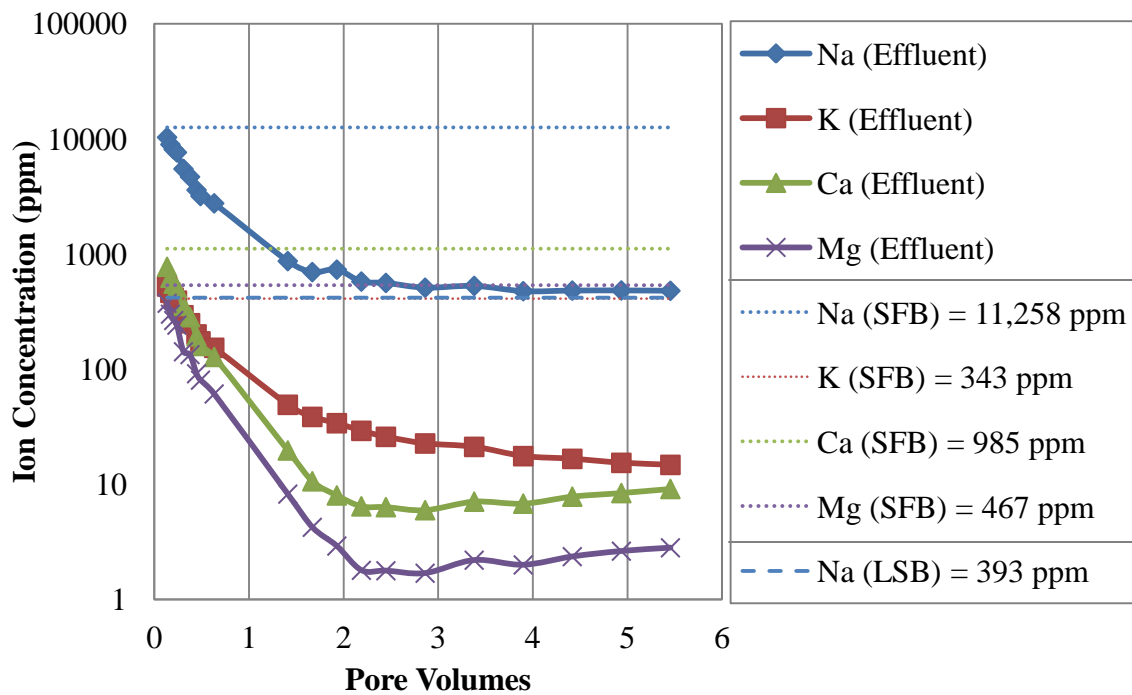


Figure 4-19: Effluent Ion Concentration of Low Salinity Waterflood 2

4.2 LOW SALINITY POLYMER FLOODING IN SEMI-TERTIARY MODE

In this experiment, a low salinity polymer flooding was conducted in semi-tertiary mode in a Berea sandstone core (Berea B). The objective of this experiment was to evaluate the effect of semi-tertiary low salinity polymer injection on residual oil saturation and effluent ion concentrations in the sandstone core.

A single core was cut from a block of visually homogeneous Berea sandstone. The Berea sandstone core with relatively low permeability was chosen because the low-perm cores tend to have more clays. A synthetic formation brine (SFB) with 33,793 ppm TDS was used as high salinity water. A low salinity polymer (LSP) solution was made by diluting SFB by 10 times and mixing with 2,500 ppm of Flopaam 3330S. Properties of the core and fluids are given in Table 4-3 and 4-4, respectively. Figure 4-20 displays polymer viscosity versus shear rate.

Table 4-3: Berea B Core Properties

Length	(inch)	10.98
Diameter	(inch)	1.50
Bulk Volume	(ml)	317.95
Pore Volume	(ml)	57.86
Porosity	(%)	18.20
Nitrogen Permeability	(md)	137.52
Brine Permeability	(md)	83.03
Clay Content	(weight%)	5.00

Table 4-4: Experiment 4.2 Fluid Properties at 85°C and 10s⁻¹

Synthetic Formation Brine (SFB)	Salt Concentration	(ppm)	28,620	NaCl
			650	KCl
			2,710	CaCl ₂
			3,890	MgCl ₂ -6H ₂ O
			33,793	TDS
	Viscosity	(cP)	0.47	
Low Salinity Polymer (LSP)	Salt Concentration	(ppm)	2,862	NaCl
			65	KCl
			271	CaCl ₂
			389	MgCl ₂ -6H ₂ O
			3,379	TDS
	Polymer Conc.	(ppm)	2,500	3330S HPAM
Viscosity	(cp)	10		
Crude Oil (Crude A)	Viscosity	(cP)	12	

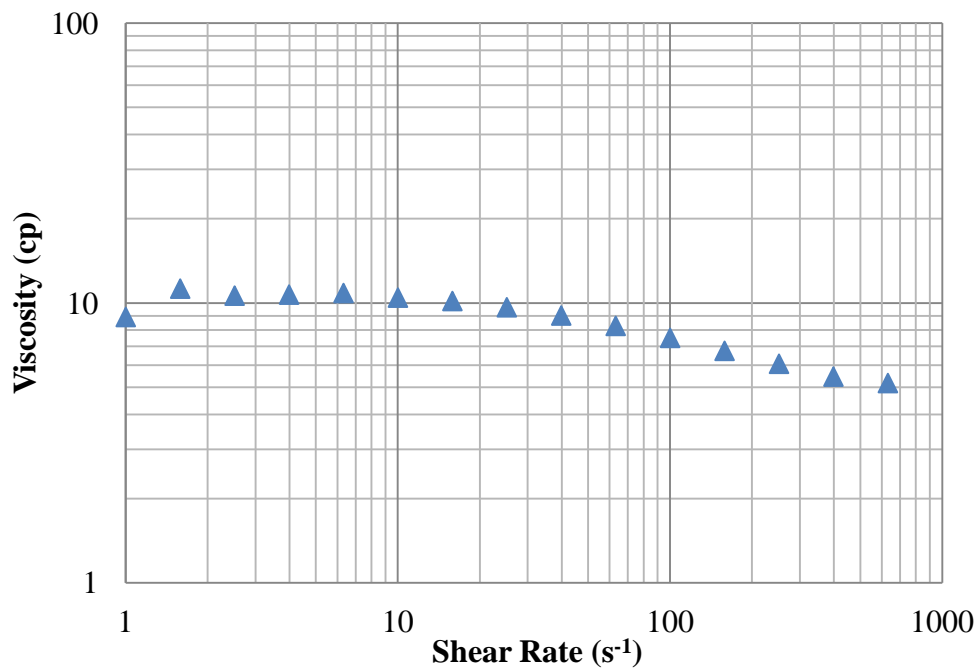


Figure 4-20: Polymer Viscosity vs. Shear Rate (T = 85°C)

After the routine core analysis procedure (described in Chapter 3), the following floods were conducted: two oil floods (Oil Flood 1-2), one water flood (High Salinity Waterflood), one polymer flood (Low Salinity Polymer Flood), and two tracer tests (Tracer Test 1-2). Figure 4-21 shows a diagram of the experimental procedure. Synthetic Formation Brine (SFB) of 0.4 PV was injected into Berea B followed by Low Salinity Polymer (LSP) until no more oil was produced and also the steady state was reached. This SFB-LSP Flood was designed based on the fractional flow curve so that polymer flood could be started when the oil cut was 80%.

Tracer Test 1	
Oil Flood 1	
30 Days Ageing @90°C	
Oil Flood 2	
High Salinity Waterflood	0.4 PV
Low Salinity Polymer Flood	3.8 PV
Tracer Test 2	

Figure 4-21: Experiment 4.2

Tracer Test 1

Tracer Test 1 was conducted at a flow rate of 0.5 mL/min to determine the pore volume of Berea B. Effluent samples were collected every 10 minutes with sample size of 5 mL. The measured conductivity was normalized on a scale of zero to one and plotted against the injected volume (Fig. 4-22). The calculated pore volume was 57.86 mL.

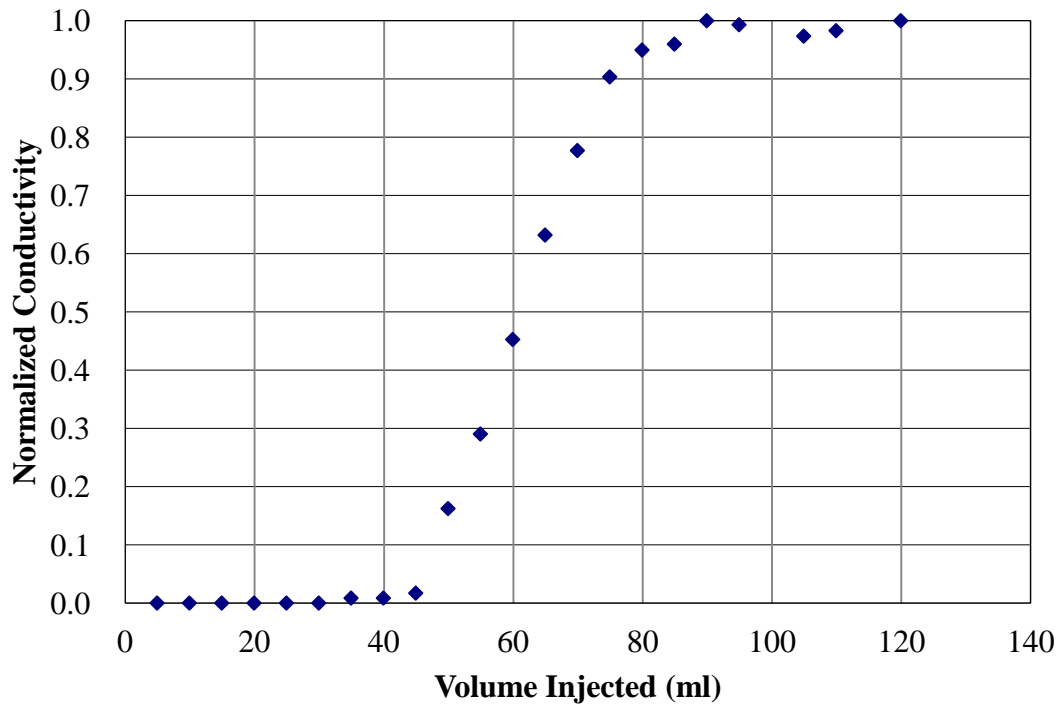


Figure 4-22: Effluent Conductivity History for Berea B (Tracer Test 1)

Oil Flood 1

Oil Flood 1 was performed using Crude A at 85°C. The oil flood was performed at a constant pressure of 200 psi. Once the pressure drop across the core reached a steady state, end point oil relative permeability k_{ro}^o was calculated to be 0.53. The value of S_{oi} was determined by mass balance and came out to be 76.0 %.

30 Days Aging

After Oil Flood 1, the core was taken out of the core holder and placed in a glass column filled with Crude A. The core was entirely immersed in oil and the column was sealed. The core was aged for 30 days at aging temperature, 90°C.

Oil Flood 2

After aging, Berea B was flooded with Crude A at a flow rate of 0.5 ml/min for 1.5PV to flush out the oil inside the core. No water was produced during the flood. Once the pressure drop across the core reached steady state, k_{ro}^o was calculated to be 0.48. This oil permeability reduction indicated wettability alteration towards oil-wet.

High Salinity Water - Low Salinity Polymer Flood

A secondary waterflood using SFB was performed followed by LSP Flood. SFB was injected at a flow rate of 0.05 mL/min (1.14 ft/Day) for 0.4 PV and LSP was injected at the same rate for 3.8 PV. The pressure drop across the core was monitored during the flood (Fig. 4-23) and the maximum pressure was 150 psi. This pressure drop was too high and not realistic to apply in the fields.

Figure 4-24 shows oil recovery, oil cut and average oil saturation versus pore volumes. Water breakthrough occurred early at 0.11PV. Oil production stopped after around 1.5PV of polymer injection and final oil recovery was 59.0%OOIP. The residual oil saturation S_{or} was determined by mass balance and came out to be 31%. This S_{or} value was the lowest among other waterfloods and polymer floods.

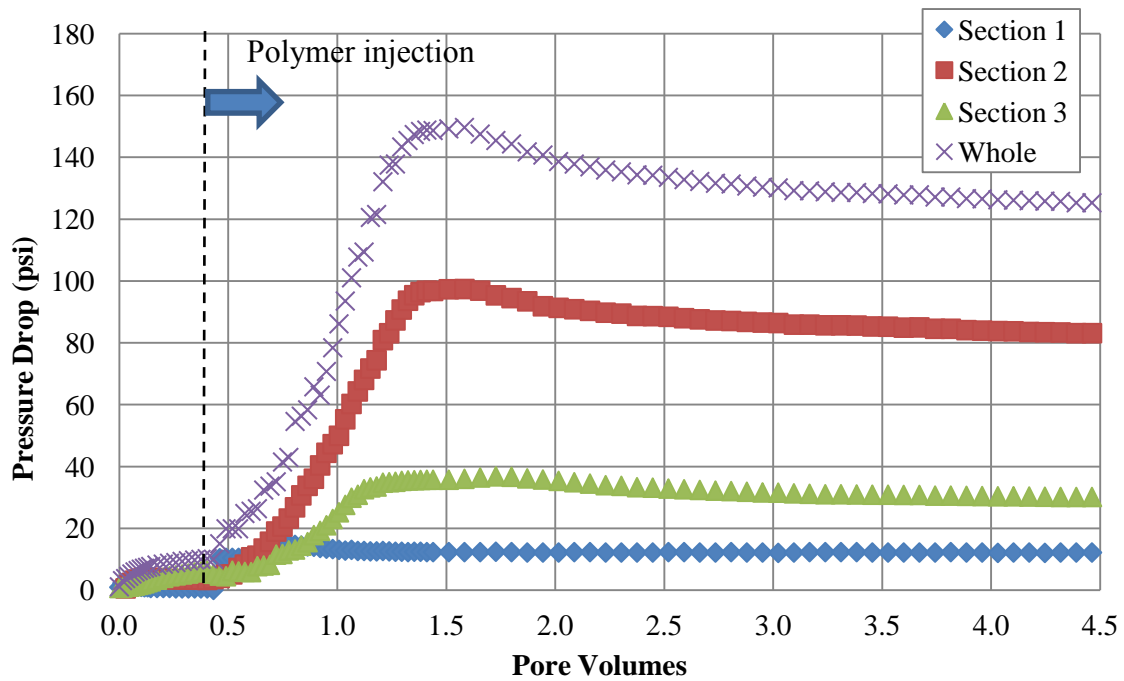


Figure 4-23: High Salinity Water – Low Salinity Polymer Flood Pressure Drop

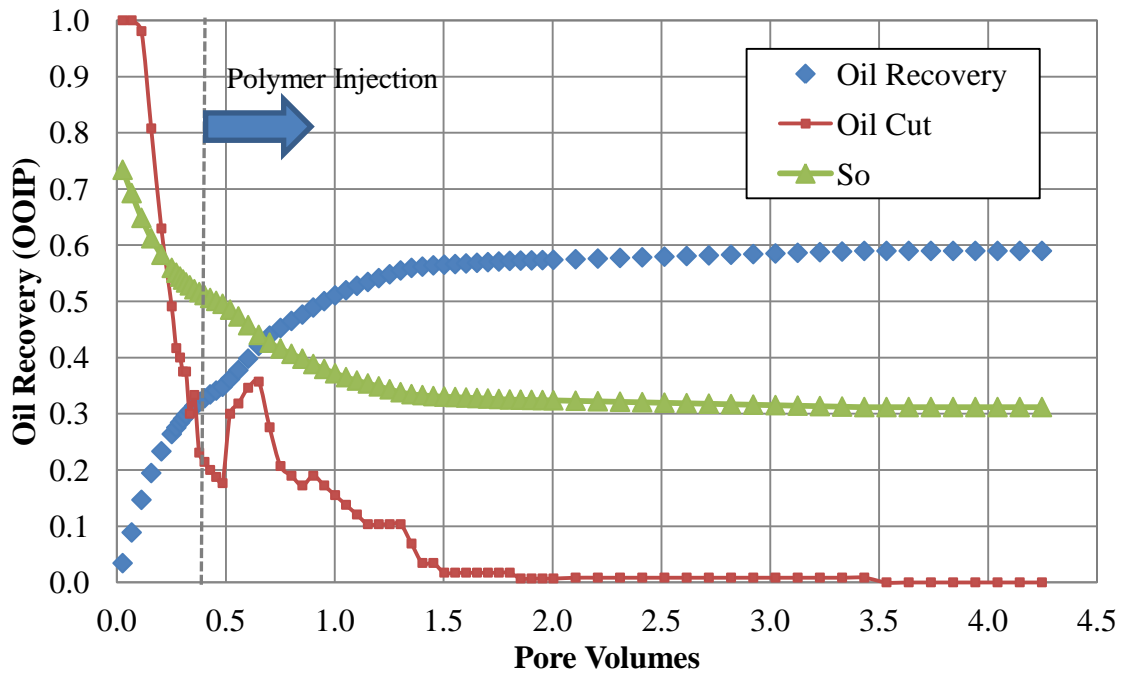


Figure 4-24: High Salinity Water – Low Salinity Polymer Flood Oil Recovery

Effluent Analysis

pH measurements and ion analysis were carried out on the effluent samples. Figure 4-25 shows effluent pH history versus pore volumes. After polymer injection started, pH increased slightly for about 1 PV and then stabilized at pH=7.3. No pH variation reported by some researchers in low salinity brine floods (Tang and Morrow, 1999, McGuire *et al.*, 2005) was observed. Thus an alkaline-like-waterflood due to high pH did not contribute to the increase in oil recovery in this case.

Figure 4-26 displays the effluent profiles for Na^+ , K^+ , Ca^{2+} , and Mg^{2+} . The dotted lines and dashed lines represent ion concentrations of connate water (SFB) and injected fluid (LSP) respectively. It can be seen that the connate water was displaced by LSP after LSP injection of about 1PV and it was almost piston-like displacement. The concentrations of Ca^{2+} and Mg^{2+} in effluents showed a slight increase after they reached the bottom while the concentrations of Na^+ and K^+ continued to decrease. The same phenomena were observed in low salinity waterfloods and it clearly shows the evidence of cation exchange between the core surfaces and low salinity fluids. However, the increase in these divalent cations began after oil production ceased almost zero.

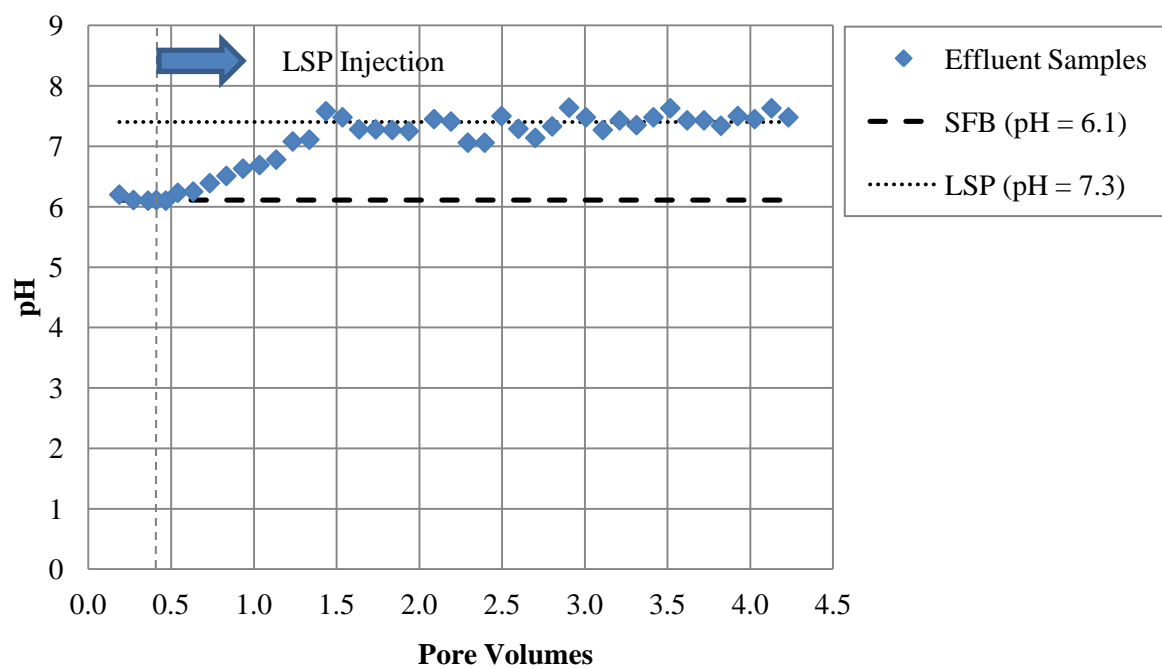


Figure 4-25: pH Profile of Experiment 4.2

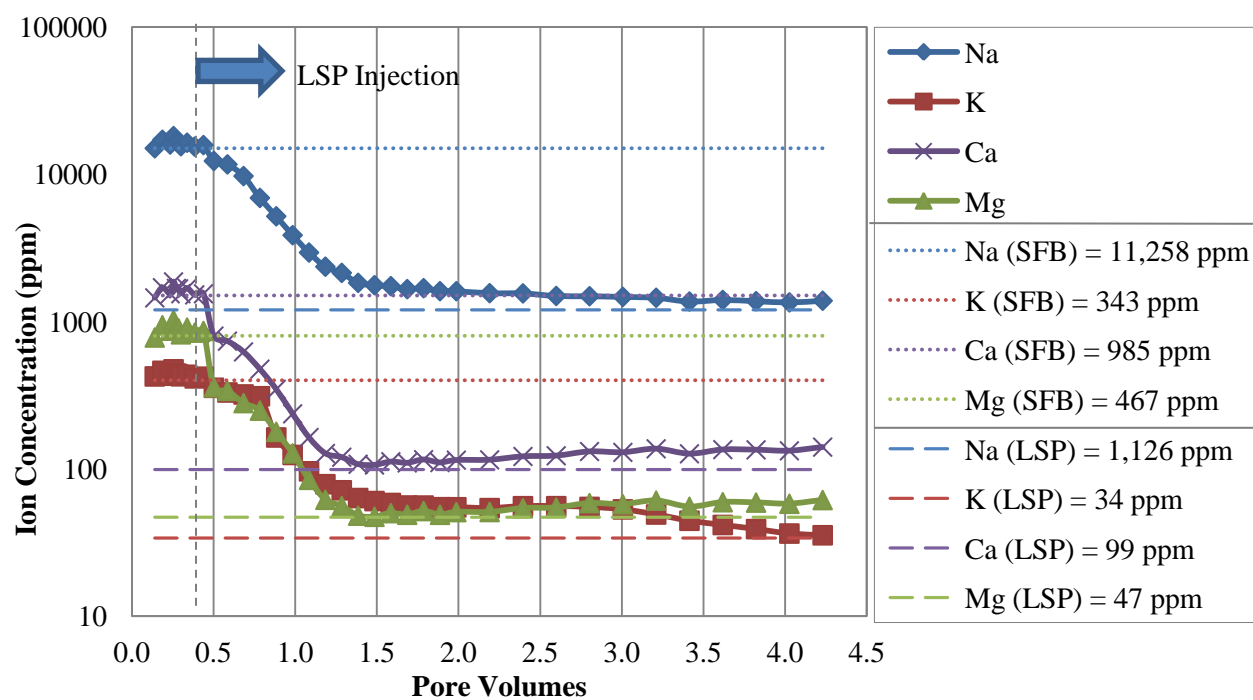


Figure 4-26: Effluent Ion Concentration of Experiment 4.2

4.3 LOW SALINITY POLYMER FLOODING IN TERTIARY MODE

In this experiment a low salinity polymer flooding were conducted in tertiary mode in a Berea sandstone core (Berea C). The objective of this experiment was to evaluate the effect of tertiary low salinity polymer injection on residual oil saturation and effluent ion concentrations in the sandstone core.

A single core was cut from a block of visually homogeneous Berea sandstone. The Berea sandstone core with relatively low permeability was chosen because the low-perm cores tend to have more clays. The same brine and polymer solution as those used in Section 4.2 were used and their properties are shown in Table 4-4. Properties of the core are given in Table 4-5.

Table 4-5: Berea C Core Properties

Length	(inch)	11.55
Diameter	(inch)	1.45
Bulk Volume	(ml)	312.53
Pore Volume	(ml)	55.50
Porosity	(%)	17.76
Nitrogen Permeability	(md)	125.95
Brine Permeability	(md)	69.40
Clay Content	(weight%)	5.00

After the core analysis procedure described in Chapter 3, the following floods were conducted: two oil floods (Oil Flood 1-2), one water flood (High Salinity Waterflood), one polymer flood (Low Salinity Polymer Flood), and two tracer tests (Tracer Test 1-2). Figure 4-27 shows a diagram of the experimental procedure. Synthetic Formation Brine (SFB) was injected into Berea C all the way till no more oil was produced and pressure stabilized. After that, Low Salinity Polymer (LSP) flood was conducted in tertiary mode till oil production stopped and steady state was reached.

Tracer Test 1	
Oil Flood 1	
30 Days Ageing @90°C	
Oil Flood 2	
High Salinity Waterflood	4.5 PV
Low Salinity Polymer Flood	4.6 PV
Tracer Test 2	

Figure 4-27: Experiment 4.3

Tracer Test 1

Tracer Test 1 was conducted at a flow rate of 0.5 mL/min to determine the pore volume of Berea C. Effluent samples were collected every 10 minutes with sample size of 5 mL. The measured conductivity was normalized on a scale of zero to one and plotted against the injected volume (Fig. 4-28). The calculated pore volume was 55.5 mL.

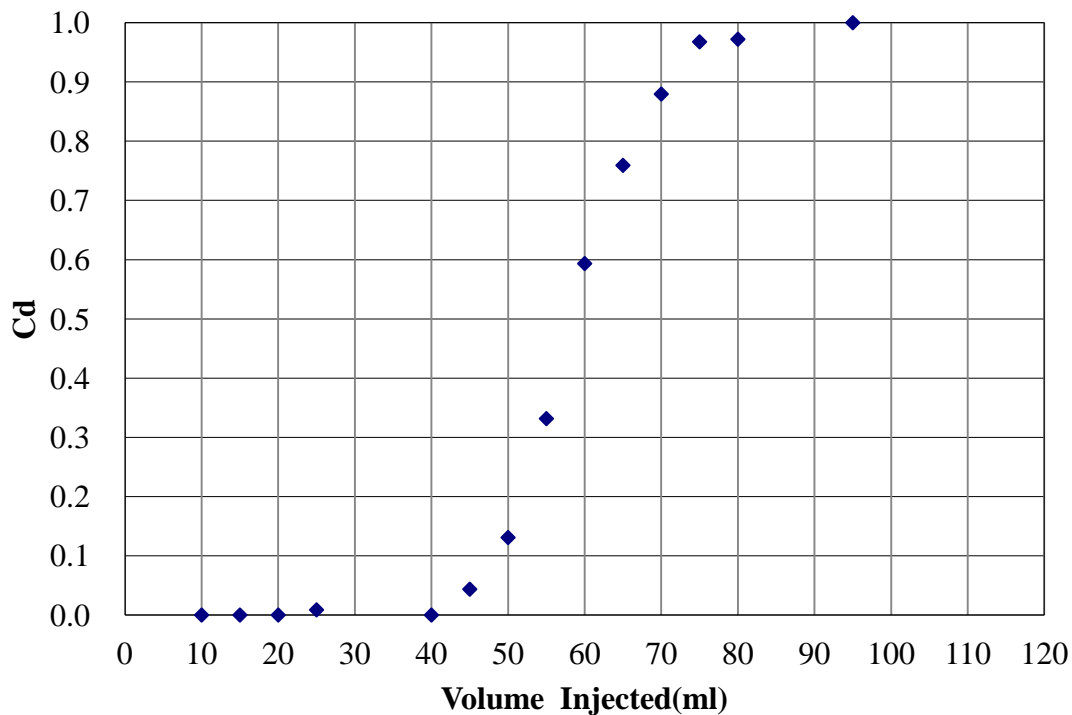


Figure 4-28: Effluent Conductivity History for Berea C (Tracer Test 1)

Oil Flood 1

Oil Flood 1 was performed using Crude A at 85°C. The oil flood was performed at a constant pressure of 200 psi. Once the pressure drop across the core reached steady state, end point oil relative permeability k_{ro}^o was calculated to be 0.71. The value of S_{oi} was determined by mass balance and came out to be 83.0 %.

30 Days Aging

After Oil Flood 1, the core was taken out of the core holder and placed in a glass column filled with Crude A. The core was entirely immersed in oil and the column was sealed. The core was aged for 30 days at aging temperature, 90°C.

Oil Flood 2

After aging, Berea C was flooded with Crude A at a flow rate of 0.5 ml/min for 2.0PV to flush out the oil inside the core. No water was produced during the flood. Once the pressure drop across the core reached steady state, k_{ro}^o was calculated to be 0.62. This oil permeability reduction indicated wettability alteration toward oil-wet.

High Salinity Water - Low Salinity Polymer Flood

A secondary waterflood using SFB was performed at a flow rate of 0.05 mL/min (1.14 ft/Day) for 2.6 PV and then flow rate was elevated to 0.1 mL/min (2.28 ft/Day). After total injection volume of 4.6 PV, LSP injection started in tertiary mode at a flow rate of 0.05 mL/min. Fig. 4-29 shows the pressure drop of each section. The maximum pressure drops across the core during waterflood and polymer flood were 15.7 psi and 124 psi respectively.

Figure 4-30 shows oil recovery, oil cut and average oil saturation. Water breakthrough occurred at 0.24PV and oil production stopped after around 2.4PV of water injection. Final oil recovery and residual oil saturation S_{or} after waterflood was 51.3%OOIP and 40.4%. Injection of low salinity polymer recovered 8% additional oil and reduced S_{or} by 6.7%. Final oil recovery was achieved after around 1PV of polymer injection.

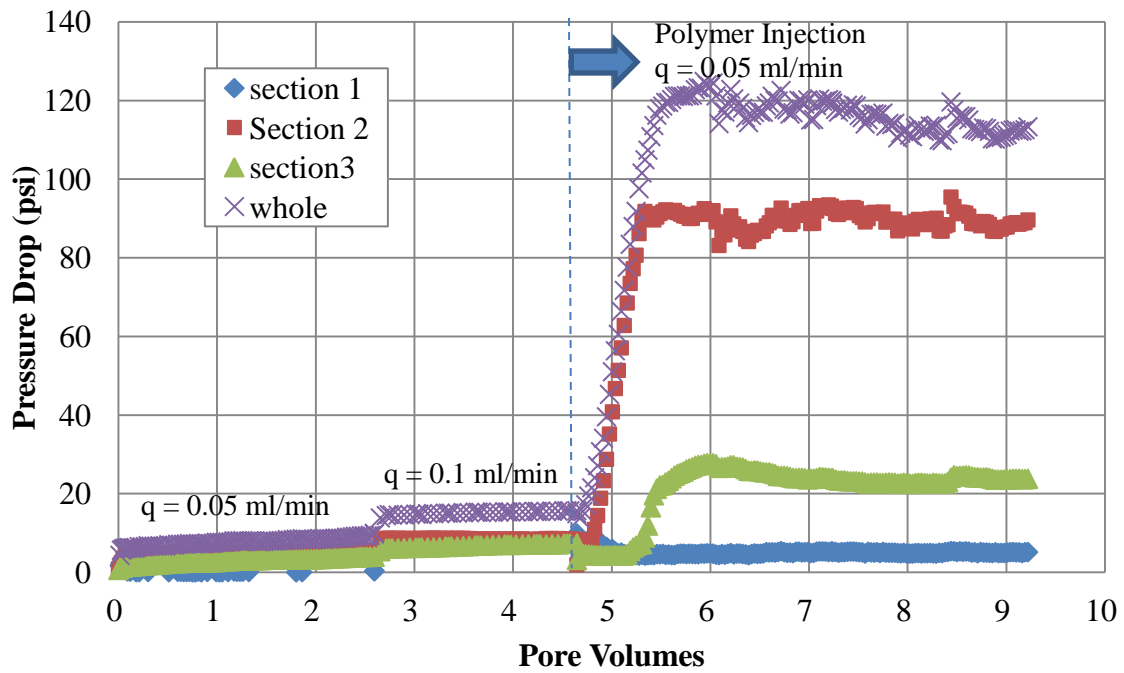


Figure 4-29: High Salinity Water – Low Salinity Polymer Flood Pressure Drop

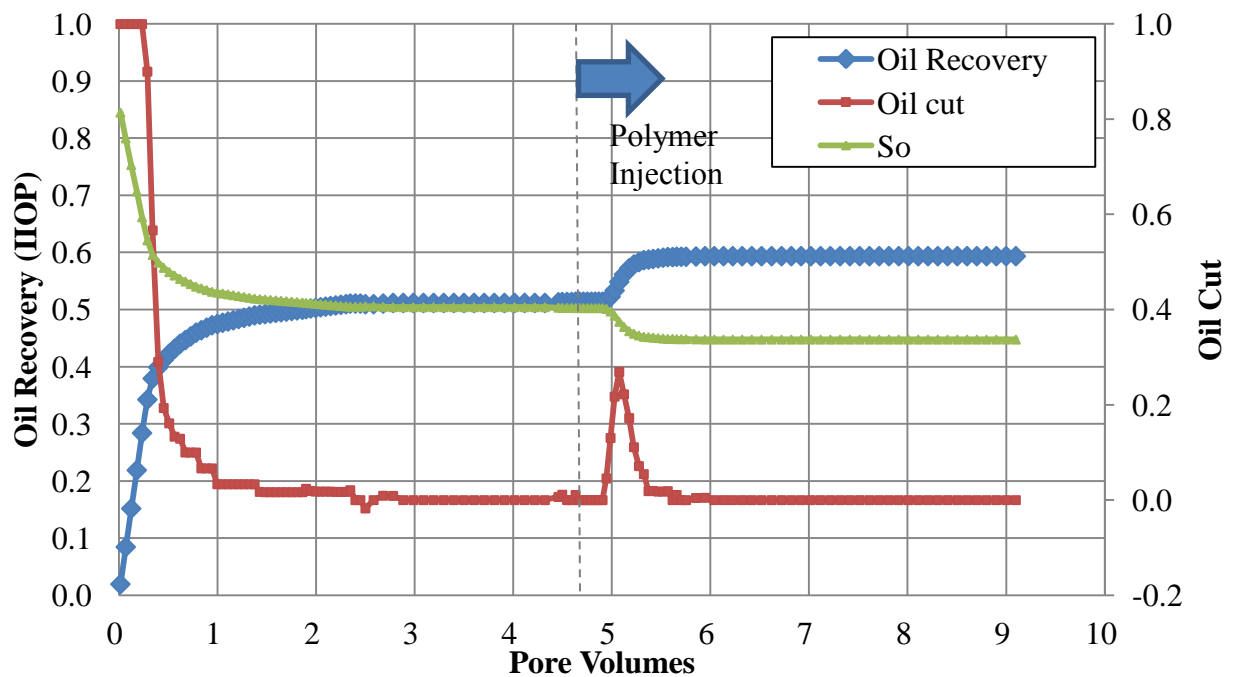


Figure 4-30: High Salinity Water – Low Salinity Polymer Flood Oil Recovery

Effluent Analysis

pH measurements and ion analysis were carried out on the effluent samples. Figure 4-31 shows effluent pH history versus pore volumes. A sharp rise in pH was observed after start of polymer injection although pH did not reach high enough to achieve an alkaline waterflood.

Figure 4-32 displays the effluent profiles for Na^+ , K^+ , Ca^{2+} , and Mg^{2+} . The dotted lines and dashed lines represent ion concentrations of connate water (SFB) and injected fluid (LSP) respectively. It can be seen that the connate water was displaced by LSP after LSP injection of about 1PV and it was almost piston-like displacement. The concentrations of Ca^{2+} and Mg^{2+} in effluents showed a slight increase after they reached the bottom. The concentration of Mg^{2+} dropped even lower than that of LSP. The similar phenomena were observed in low salinity waterfloods (Experiment 4.1) and low salinity polymer flood in semi-tertiary mode (Experiment 4.2). It again shows the evidence of cation exchange between the core surfaces and low salinity fluids. In this case also, the increase in these divalent cations began after oil production rate reached almost zero.

Figure 4-33 shows effluent viscosity history versus volume of polymer injected. There is no evidence of polymer degradation observed.

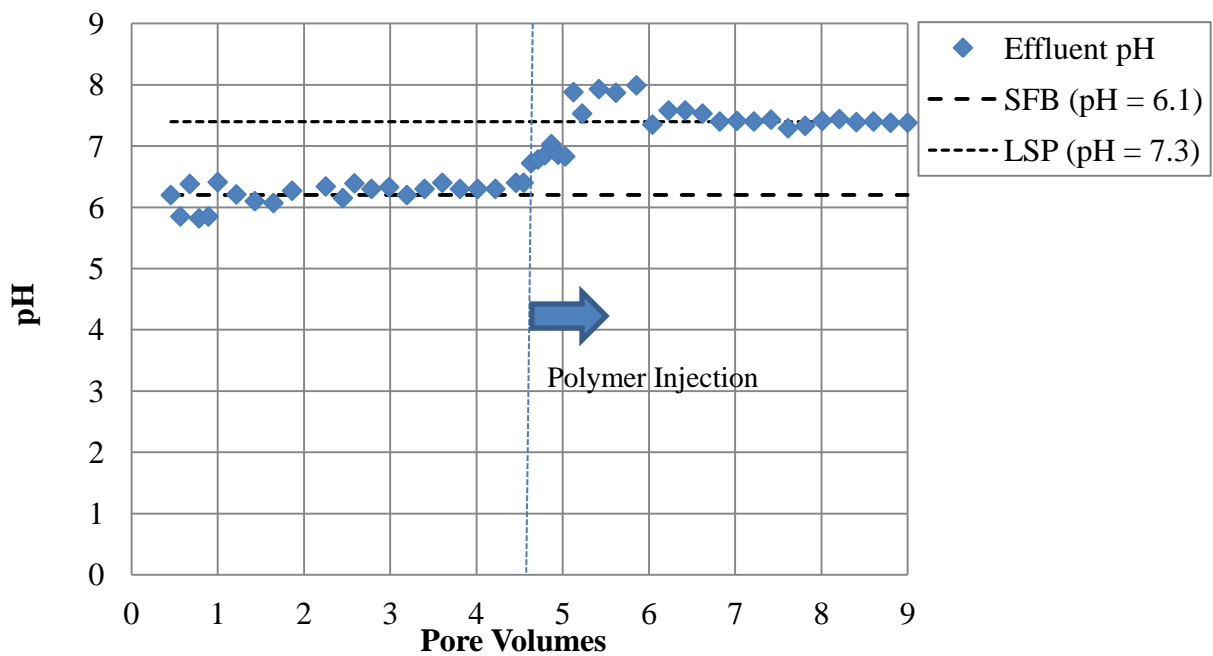


Figure 4-31: pH Profile of Experiment 4.3

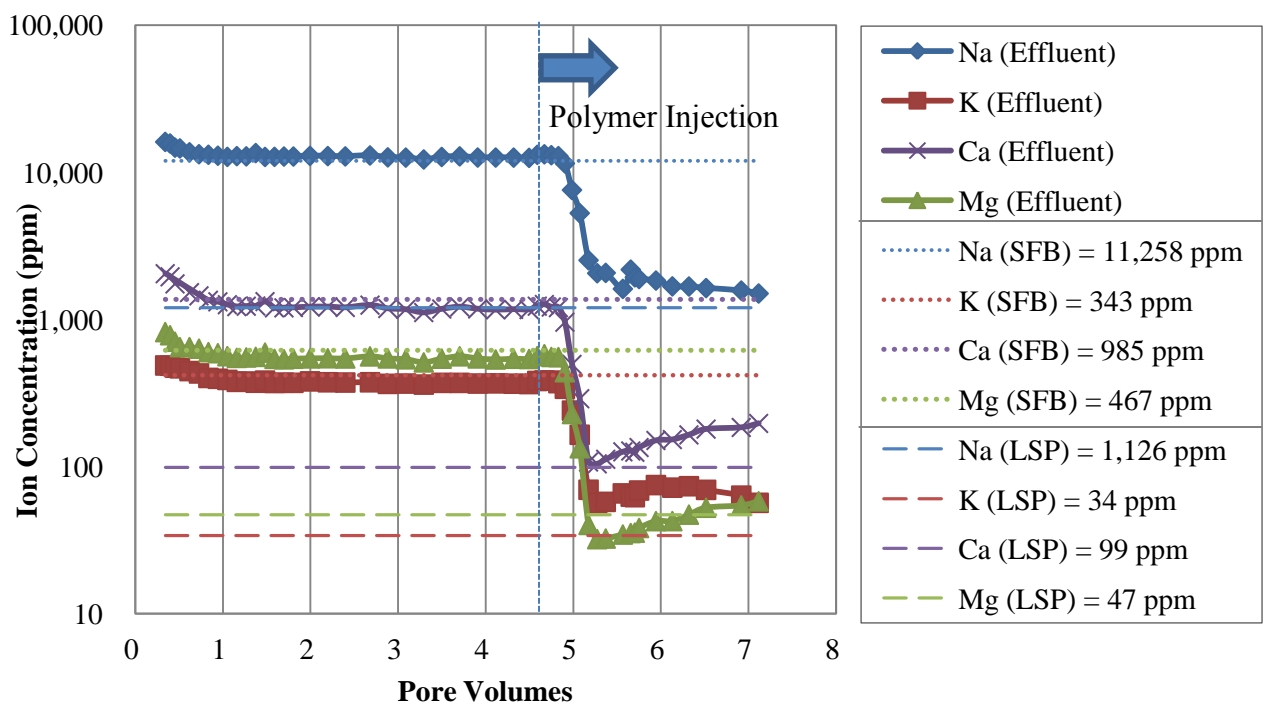


Figure 4-32: Effluent Ion Concentration of Experiment 4.3

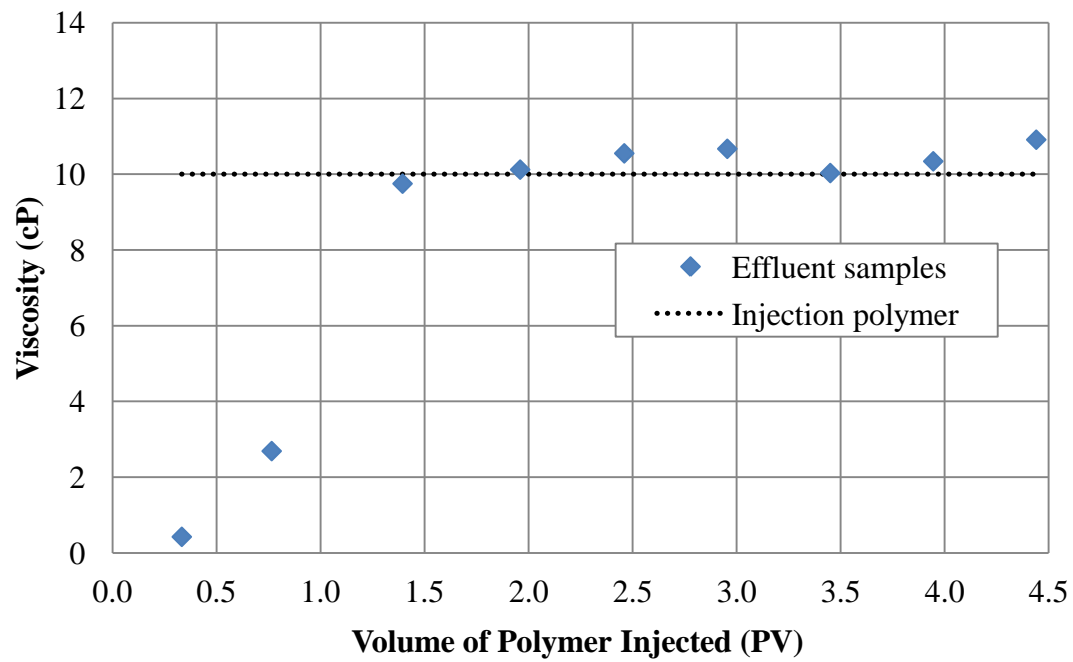


Figure 4-33: Effluent Viscosity of Experiment 4.3

CHAPTER 5: SUMMARY AND CONCLUSIONS

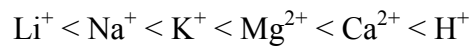
This study was undertaken to investigate the efficiency of low salinity water flooding and low salinity polymer flooding in sandstone cores. Three sets of core flood experiments were conducted: secondary waterfloods in Berea A, semi-tertiary polymer flood in Berea B, and tertiary polymer flood in Berea C.

In Experiment 4.1, two high salinity secondary and two low salinity secondary waterfloods were conducted. Table 5.1 summarizes residual oil saturations and end point relative permeabilities. All the oil recovery curves are shown in Figure 5.1. In all of the waterfloods, 2.0~2.5 pore volumes of water injection were required to reach the ultimate oil recovery. Although Berea A showed some differences between two cycles of high salinity waterfloods, injection of low salinity water gave more oil recovery than high salinity water in both cases. It may be because more aging time made core more oil-wet. Also the first injection of low salinity water might have changed core properties permanently and thus the core reacted in the different manner. The possible change in the characteristic of the core after exposure to low salinity water was also reported by Loahardjo *et al.* (2007). In their study, after low salinity flooding, re-aged cores gave increased recovery for injection of high salinity brine, which differs from our results. Because of the complexity of crude oil/brine/rock interactions, it is difficult to compare and reproduce the results from one flood cycle to the next.

In Experiment 4.2 and 4.3, a low salinity semi-tertiary polymer flood and a tertiary polymer flood were performed. Residual oil saturations and oil recoveries are summarized in Table 5.3 and oil recovery curves are shown in Figure 5.2. The low-perm Berea sandstone cores used in this study were clearly poor candidates for low salinity

polymer flood because unfavorably high pressure drop was observed during the flood. However injection of low salinity polymer solution reduced residual oil saturation by maximum of 10% over that of the high salinity waterflood. The ultimate oil recovery was achieved with less pore volumes of injection (~1.5PV) than that in waterfloods. Results also showed that injection of polymer at an earlier stage of flooding decreased residual oil saturation slightly more.

From results of effluent ion analysis, we can see that increasing amounts of divalent cations such as Ca^{2+} and Mg^{2+} were produced after extra oil recovery. It can be assumed that divalent cations were strongly adsorbed on to the negatively charged core surface during high salinity flood and then low salinity solution flushed out those ions by destabilizing the bonds between divalent cations and its surroundings. The relative ease of replacement of one cation by another is:



According to Buckley *et al.*, specific interactions between charged sites of the rock surface and higher valency ions promote wettability alteration towards less water-wet state. In this study, further production of divalent cations was observed after oil production rate reached almost zero. A possible explanation for the phenomenon is that the flow rate of divalent cations was slowed by repeatedly adsorbing and desorbing from the rock surface while oil particles released from the surface with those ions moved towards the outlet.

The most important observation of this research is that the beneficial effects of low salinity polymer flooding in tertiary/semi-tertiary mode were observed. Further investigation is required to identify the responsible mechanism(s) and to analyze synergy of low salinity water flooding and low salinity polymer flooding. Simulation work would be helpful to predict and confirm the results from core flood tests.

Table 5-1: End Point Relative Permeability of Experiment 4.1

	So	k _{ro}	k _{rw}
Oil Flood 1	78.0%	0.57	
Oil Flood 2	78.0%	0.45	
High Salinity Water 1	38.7%		0.026
Oil Flood 3	74.0%	0.48	
Low Salinity Water 1	34.7%		0.013
Oil Flood 4	81.0%	0.54	
Oil Flood 5	81.0%	0.36	
High Salinity Water 2	44.4%		0.020
Oil Flood 6	79.0%	0.34	
Low Salinity Water 2	39.7%		0.020

Table 5-2: Results Summary of Experiment 4.1

	High Salinity Waterflooding 1	Low Salinity Waterflooding 1	High Salinity Waterflooding 2	Low Salinity Waterflooding 2
Initial Oil Saturation	78%	74%	81%	79%
Residual Oil Saturation	38.7%	34.7%	44.4%	39.7%
Oil Recovery	50.3% OOIP	53.2 % OOIP	45.2% OOIP	49.7% OOIP

Table 5-3: Results Summary of Experiment 4.2 and 4.3

	LSP 1	LSP 2
Initial Oil Saturation	76%	83%
Residual Oil Saturation	31%	33%
Oil Recovery	59% OOIP	60% OOIP

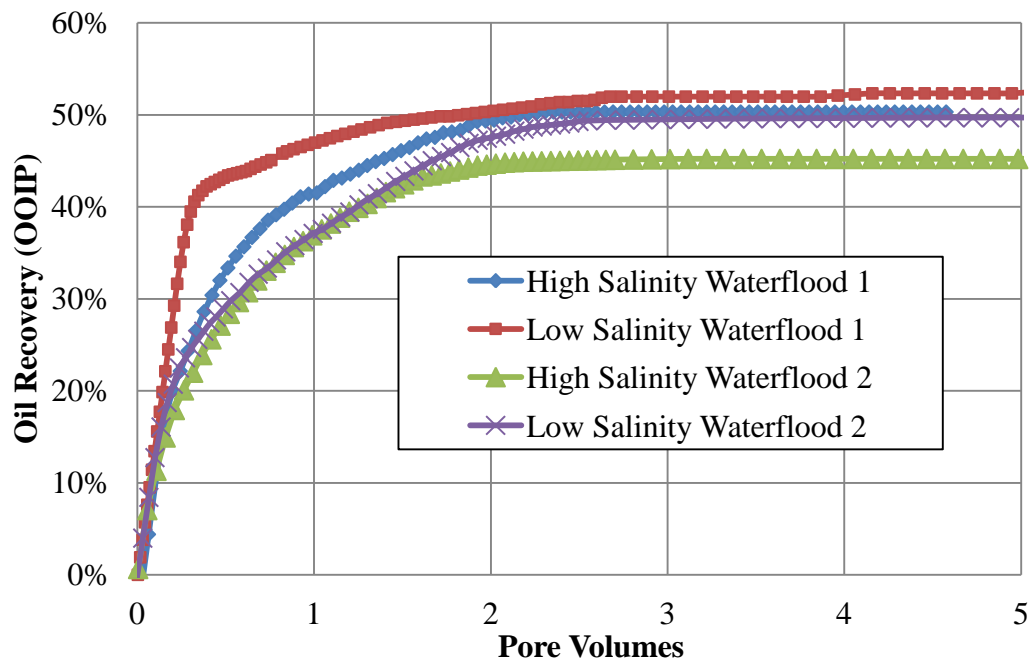


Figure 5-1: Oil Recovery Curves from Experiment 4.1

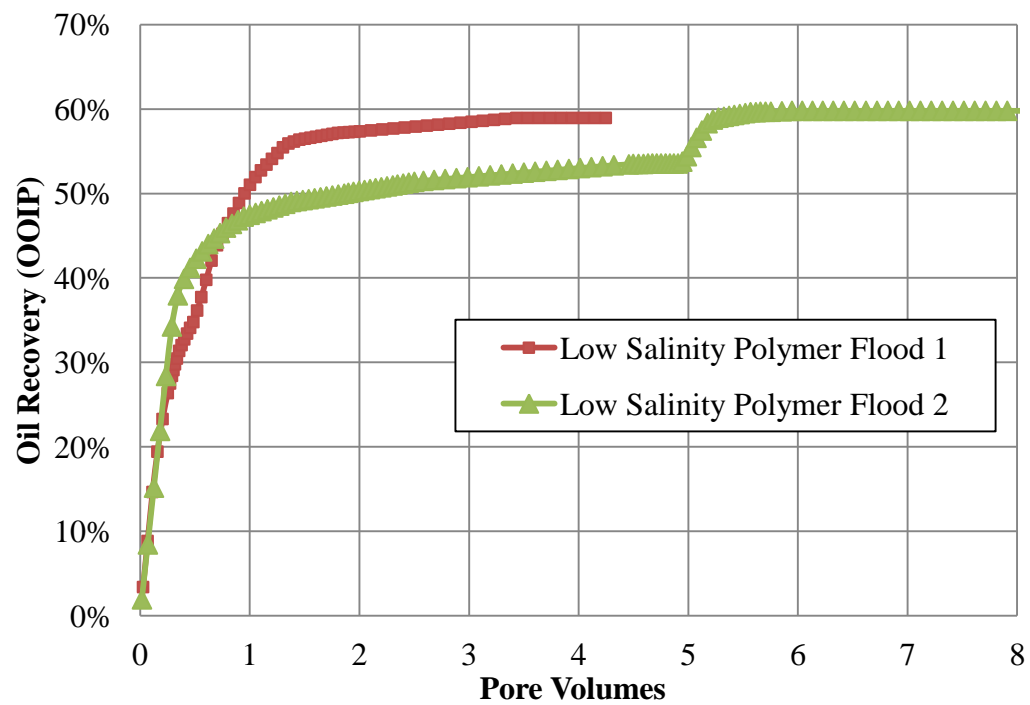


Figure 5-2: Oil Recovery Curves from Experiment 4.2 and 4.2

Appendix

This section provides a summary of the coreflood experiment (Experiment A) not included in the main body of this thesis.

Table A-1: Berea D Core Properties

Length	(inch)	11.55
Diameter	(inch)	1.47
Bulk Volume	(ml)	321.21
Pore Volume	(ml)	62.00
Porosity	(%)	19.30
Nitrogen Permeability	(md)	139.98
Brine Permeability	(md)	72.83
Clay Content	(weight%)	5.00

Table A-2: Experiment A Fluid Properties at 85°C and 10s⁻¹

Synthetic Formation Brine (SFB)	Salts Concentration	(ppm)	28,620	NaCl
			650	KCl
			2,710	CaCl ₂
			3,890	MgCl ₂ -6H ₂ O
			33,793	TDS
	Viscosity	(cP)	0.47	
Low Salinity Brine (LSB)	Salts Concentration	(ppm)	1,000	NaCl
			1,000	TDS
	Viscosity	(cP)	0.47	
Low Salinity Polymer-II (LSP-II)	Salts Concentration	(ppm)	1,000	NaCl
			1,000	TDS
	Polymer Conc.		1,000	3630S
	Viscosity	(cP)	12.8	
Crude Oil (Crude A)	Viscosity	(cP)	12	

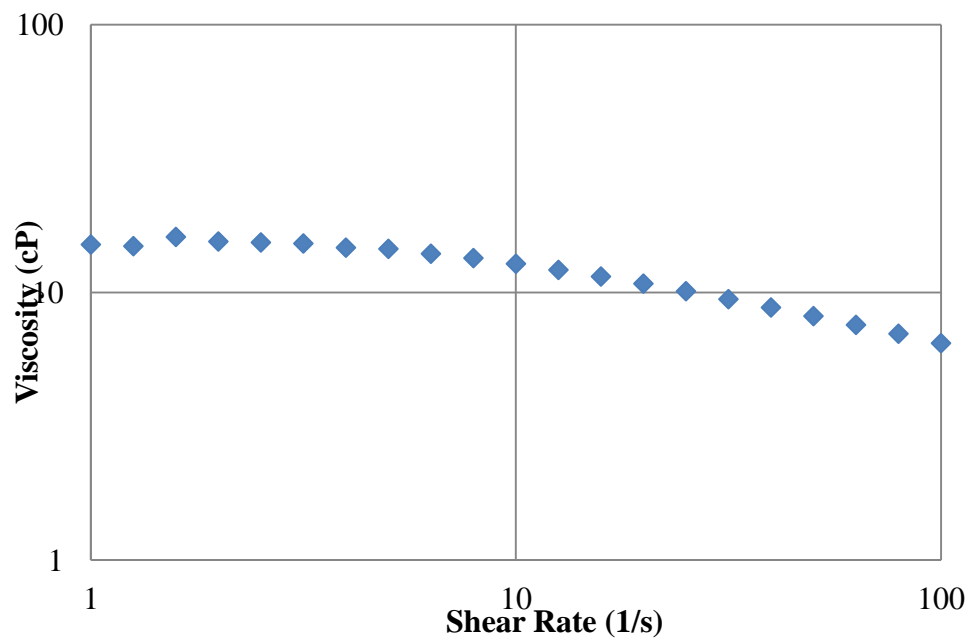


Figure A-1: Polymer Viscosity vs. Shear Rate (T = 85°C)

Tracer Test 1	
Oil Flood 1	
30 Days Ageing @90°C	
Oil Flood 2	
Low Salinity Polymer Flood	1.25 PV
Low Salinity Water Flood	4 PV
Tracer Test 2	

Figure A-2: Experiment A

Tracer Test 1

Tracer Test 1 was conducted at a flow rate of 5.0 mL/min to determine the pore volume of Berea D. Effluent samples were collected every 2 minutes with sample size of 10 mL. The measured conductivity was normalized on a scale of zero to one and plotted against the injected volume (Fig. A-3). The calculated pore volume was 62.0 mL.

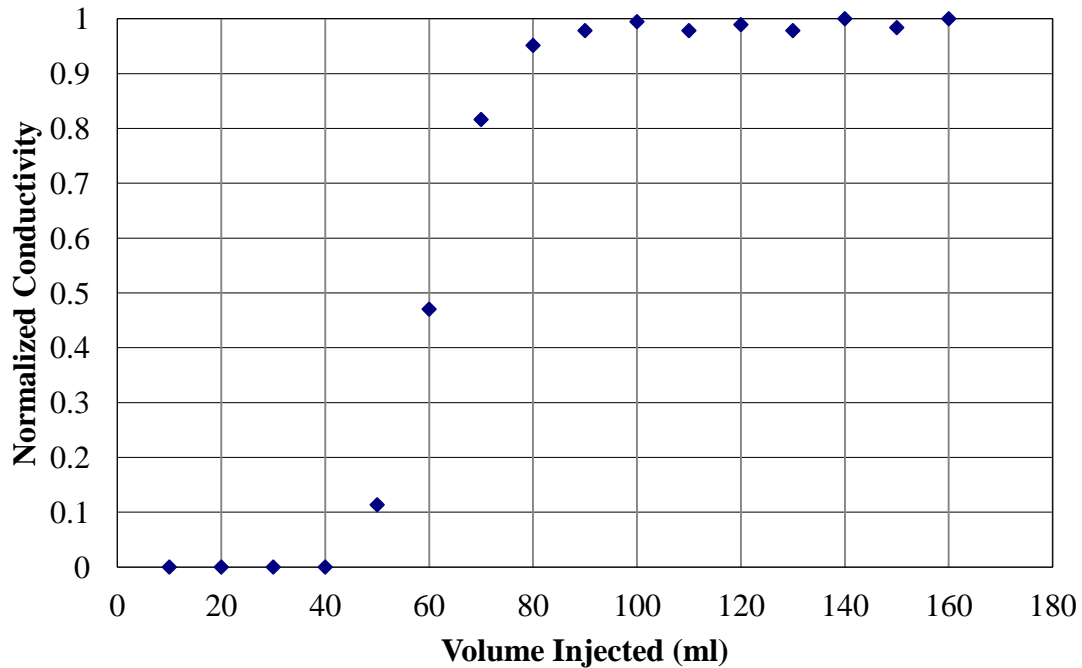


Figure A-3: Effluent Conductivity History for Berea D (Tracer Test 1)

Oil Flood 1

Oil Flood 1 was performed using Crude A at 85°C. The oil flood was performed at a constant pressure of 200 psi. Once the pressure drop across the core reached steady state, end point oil relative permeability k_{ro}^o was calculated to be 0.64. The value of S_{oi} was determined by mass balance and came out to be 76.0 %.

30 Days Aging

After Oil Flood 1, the core was taken out of the core holder and placed in a glass column filled with Crude A. The core was entirely immersed in oil and the column was sealed without leaking. The core was aged for 30 days at aging temperature, 90°C.

Oil Flood 2

After aging, Berea D was flooded with Crude A at a flow rate of 0.5 ml/min for 2PV to flush out the oil inside the core. No water was produced during the flood. Once the pressure drop across the core reached steady state, k_{ro}^o was calculated to be 0.54. This oil permeability reduction indicated wettability alteration toward oil-wet.

Secondary Low Salinity Polymer Flood

A secondary polymer flood using LSP-II was performed followed by LSB Flood. LSP-II was injected at a flow rate of 0.05 mL/min (1.1 ft/Day) for 1.25PV and LSB was injected at the same rate for 4PV. The pressure drop across the core was monitored during the flood (Fig. A-4) and maximum pressure reached only 43.8 psi. This low pressure drop indicated that low salinity polymer solution degraded under the high temperature during the flood.

Figure A-5 shows oil recovery, oil cut, and average oil saturation versus pore volumes. Water breakthrough occurred at 0.27PV of polymer injection and final oil recovery was 52%OOIP. No oil was produced during low salinity waterflooding. The residual oil saturation S_{or} was reduced to 35%, which was almost same as that obtained in Low Salinity Waterflooding 1.

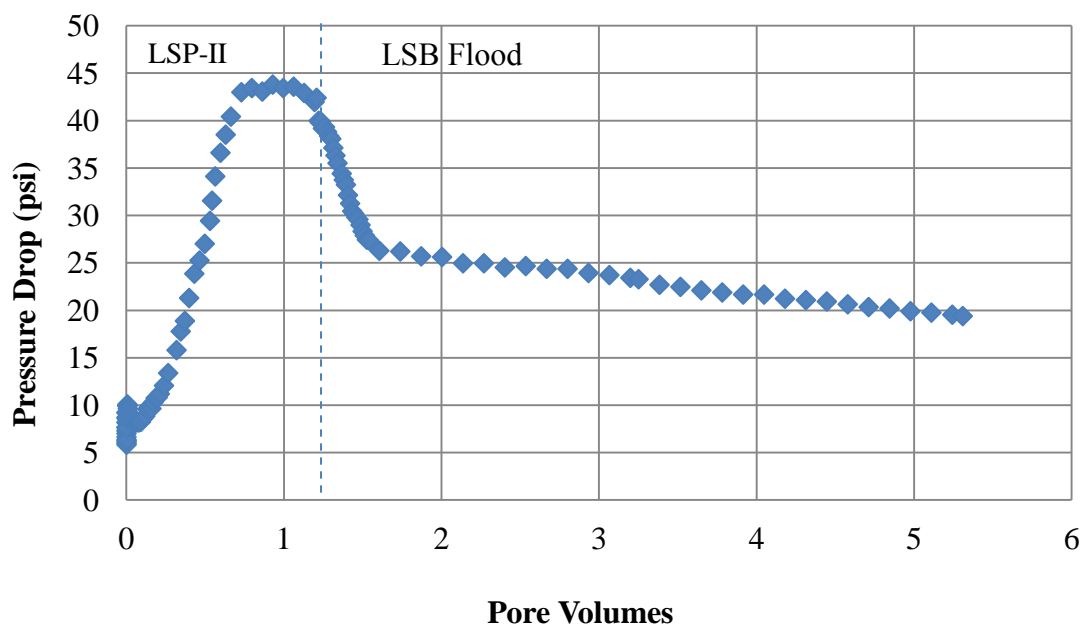


Figure A-4: Low Salinity Polymer-II – Low Salinity Water Flood Pressure Drop

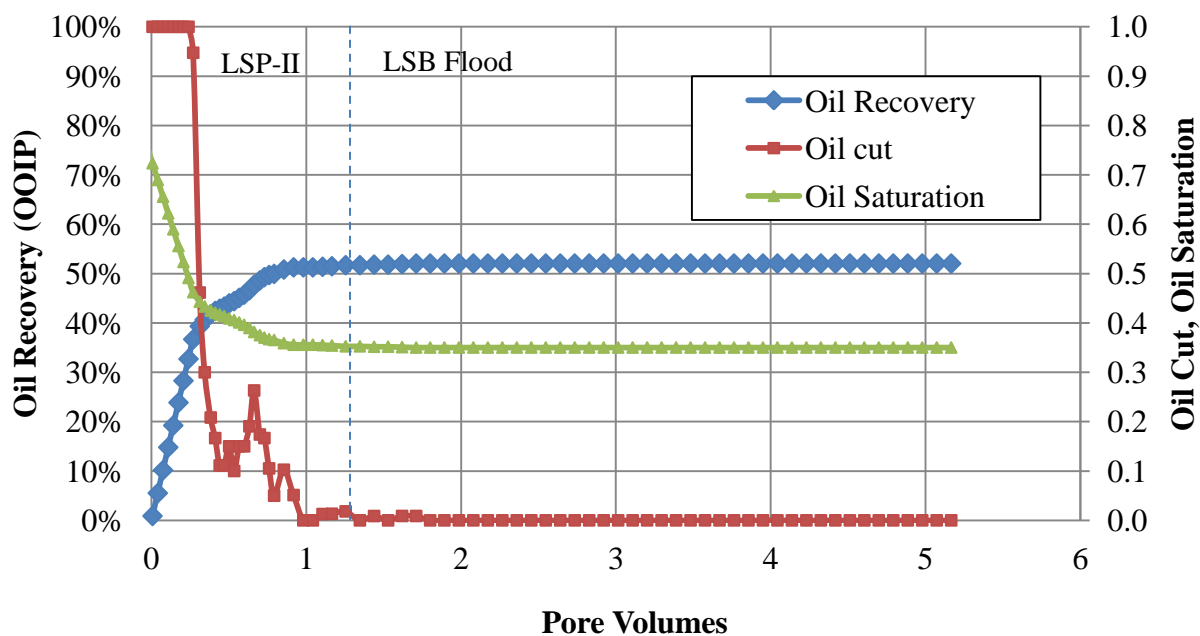


Figure A-5: Low Salinity Polymer-II – Low Salinity Water Flood Oil Recovery

Effluent Analysis

Ion analysis was carried out on the effluent samples. Figure A-6 shows the effluent profiles for Na^+ , K^+ , Ca^{2+} , and Mg^{2+} . The dotted lines and dashed lines represent ion concentrations of connate water (SFB) and injected fluid respectively. The connate water (SFB) was displaced by LSP-II after injection of about 1PV. Ca^{2+} and Mg^{2+} showed a slight increase in concentrations after 2PV. Ion concentrations of K^+ , Ca^{2+} , and Mg^{2+} did not reach zero during the flood even though injected brine had zero concentrations of these ions.

The viscosity of the effluent sample at the end of the LSP-II flood (with no oil residues) was measured to determine if LSP-II viscosity had degraded. Figure A-7 plots the end point viscosity of LSP-II flood. The polymer solution had viscosity of about 1.1 cP and it is clearly showed that degradation occurred to the polymer solution.

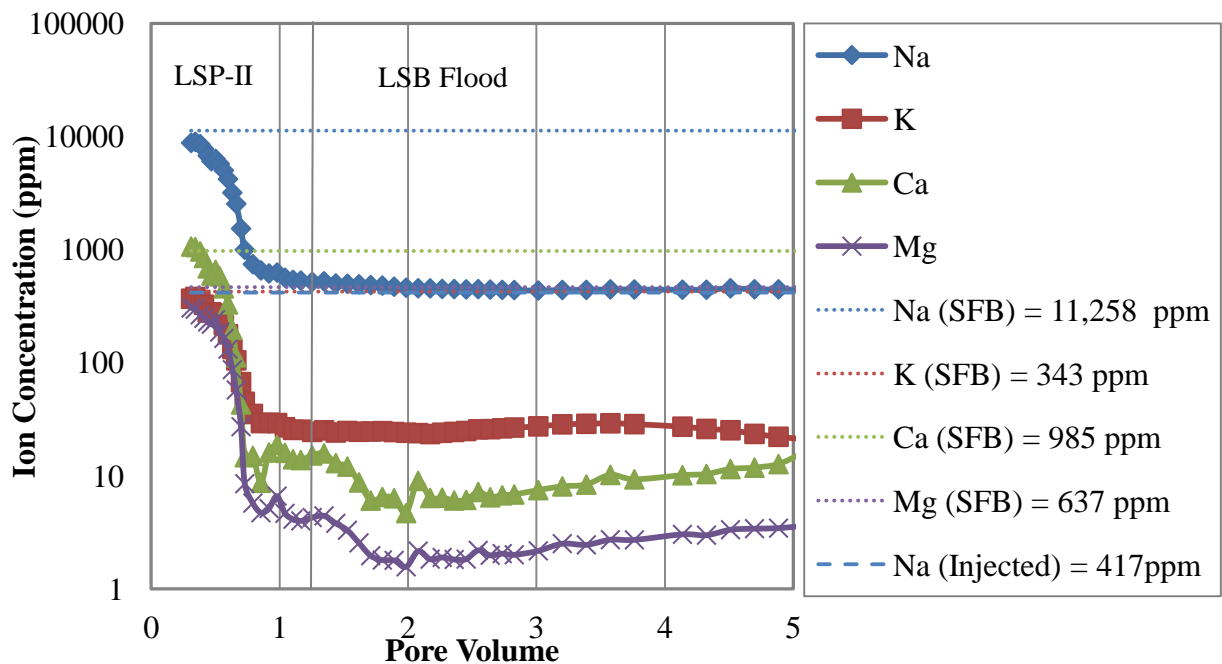


Figure A-6: Effluent Ion Concentration of Experiment A

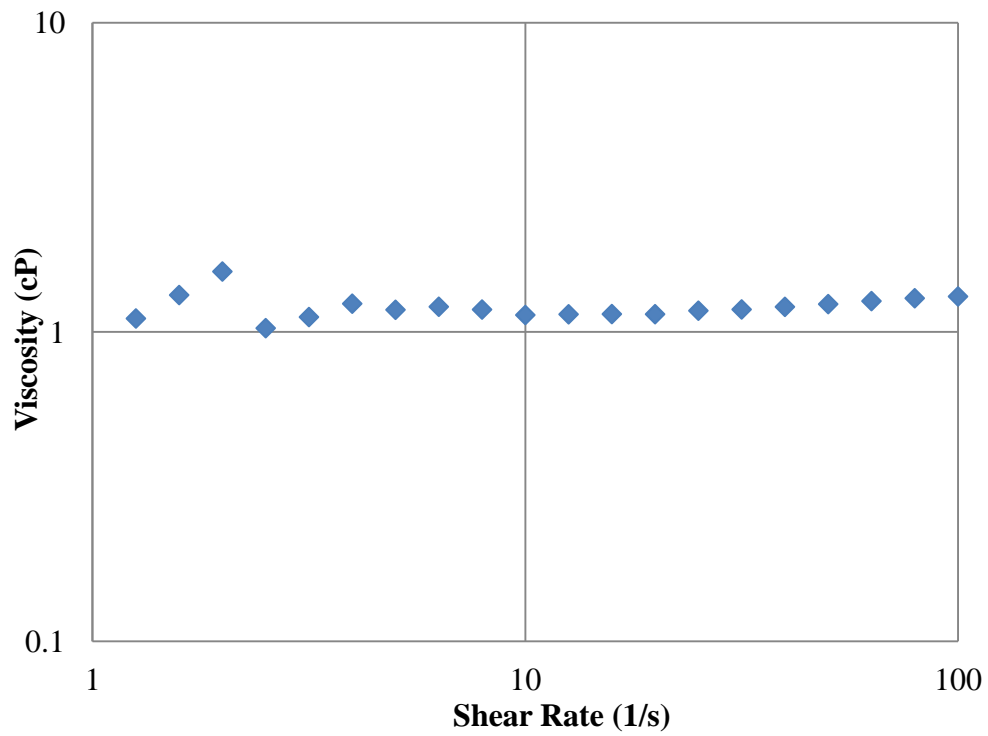


Figure A-7: End Point Effluent Viscosity of LSP-II Flood

References

- Abdallah, W. "Fundamentals of Wettability", Schlumberger Oilfield Review Vol.19, 2007.
- Agbalaka , C.C., Dandekar, A.Y., Patil, S.L., Khataniar, S., and Hemsath, J.R. "Coreflooding Studies to Evaluate the Impact of Salinity and Wettability on Oil Recovery Efficiency", Transport in Porous Media Vol. 76: 77-94, 2009.
- Alagic, E. and Skauge, A. "Combined Low Salinity Brine Injection and Surfactant Flooding in Mixed-Wet Sandstone Cores", Energy Fuels Vol. 24: 3551-3559, 2010.
- Alagic, E., Spildo, K., Skauge, A., and Solbakken, J. "Effect of Crude Oil Aging on Low Salinity and Low Salinity Surfactant Flooding", Journal of Petroleum Science and Engineering Vol. 78: 220-227, 2011.
- Anderson, G.A. "Simulation of Chemical Flood Enhanced Oil Recovery Processes Including the Effect of Reservoir Wettability", M.S. Thesis, The University of Texas at Austin, May 2006.
- Anderson, W.G. "Wettability Literature Survey-part I: Rock/oil/brine interactions and the Effect of Core Handling on Wettability", Journal of Petroleum Technology Vol.38: 1125-1144, 1986.
- Anderson, W.G. "Wettability Literature Survey-part II: Wettability Measurement", Journal of Petroleum Technology Vol.38: 1246-1262, 1986.
- Austad, T., RezaeiDoust, A., and Puntervold, T. "Chemical Mechanism of Low Salinity Water Flooding in Sandstone Reservoirs", SPE 129767, 2010.
- Ayirala, S., Ernesto, U., Matzakos, A., Chin, R., Doe, P., and van Den Hoek, P. "A Designer Water Process for Offshore Low Salinity and Polymer Flooding Applications", SPE 129926, 2010.
- Baptist, O.C. and Sweeney, S.A. "The Effect of Clays on the Permeability of Reservoir Sands to Waters of Different Saline Contents", Pacific Coast Regional Conference on Clays and Clay Technology, Berkeley, California, Jun. 25-26, 1954.
- Batias, J., Hamon, G., Lalanne, B., and Romero, C. "Field and Laboratory Observations of Remaining Oil Saturations in a Light Oil Reservoir Flooded by a Low Salinity Aquifer", presented at the International Symposium of the Society of Core Analysis in Noordwijk, Netherlands, Sep. 27-30, 2009.
- Bernard, G.G. "Effect of Floodwater Salinity on Recovery of Oil from Cores Containing Clays", SPE 1725, Los Angeles, California, Oct.26-27, 1967.

- Boussour, S., Cissokho, M., Cordier, P., Bertin, H., and Hamon, G. "Oil Recovery by Low Salinity Brine Injection: Laboratory Results on Outcrop and Reservoir Cores", SPE 124277, 2009.
- Buckley, J.S., Takamura, K., and Morrow, N.R. "Influence of Electrical Surface Charges on the Wetting Properties of Crude Oils", SPE Reservoir Engineering Vol.4: 332-340, 1989
- Dodd, C.G., Conley, F.R., and Barnes, P.M. "Clay Minerals in Petroleum Reservoir Sands and Water Sensitivity Effects", Clay and Clay Minerals Vol.3: 221-238, 1954.
- Donaldson, E.C., Thomas, R.D., and Lorenz, P.B. "Wettability Determination and Its Effect on Recovery Efficiency", SPEJ, 1969.
- Filoco, P.R. and Sharma, M.M. "Effect of Brine Salinity and Crude Oil Properties on Relative Permeabilities and Residual Saturations", SPE 49320-MS, 1998.
- Green, D.W. and Willhite, G.P. "Enhanced Oil Recovery", SPE Textbook Series Vol.6, 1998.
- Jadhunandon, P.P. and Morrow, N.R. "Effect of Wettability on Waterflood Recovery for Crude-Oil/Brine/Rock Systems", SPE 22597, 66th Annual Technical Conference, Dallas, TX, 1991.
- Jarrell, P.M., Fox, C.E., Stein, M.H., and Webb, S.L. "Practical Aspects of CO₂ Flooding", Monograph Series, SPE, 2002.
- Lager, A., Webb, K.J., Black, C.J.J., Singleton, M., and Sorbie, K.S. "Low Salinity Oil Recovery – An Experimental Investigation", paper presented at the International Symposium of the Society of Core Analysis in Trondheim, Norway, 2006.
- Lager, A., Webb, K.J., and Black, C.J.J. "Impact of Brine Chemistry on Oil Recovery", 14th European Symposium on Improved Oil Recovery, in Cairo, Egypt, Apr. 22-24, 2007.
- Lager, A., Webb, K.J., Collins, I.R., and Richmond, D.M. "LoSalTM Enhanced Oil Recovery: Evidence of Enhanced Oil Recovery at the Reservoir Scale", SPE 113976, 2008.
- Lee, S.Y., Webb, K.J., Collins, I.R., Lager, A., Clarke, S.M., O'Sullivan M., Routh, A.F., and Wang, X. "Low Salinity Oil Recovery – Increasing Understanding of the Underlying Mechanisms", SPE 129722, 2010.
- Ligthelm, D.J., Gronsveld, J., Hofman, J.P., Brussee, N.J., Marcelis, F., and van der Linde, H.A. "Novel Waterflooding Strategy by Manipulation of Injection Brine Composition", SPE 119835, 2009.
- Loahardjo, N., Xie, X., Yin, P., and Morrow, N.R. "Low Salinity Waterflooding of a Reservoir Rock", Society of Core Analysis, Sep. 2007.

- Martin, J.C. "The Effect of Clays on the Displacement of heavy Oil by Water", SPE 1411-G, Caracas, Venezuela, Oct.14-16, 1959.
- McGuire, P.L., Chatham, J.R., Paskvan, F.K., Sommer, D.M., and Carini, F.H. "Low Salinity Oil Recovery: An Exciting New EOR Opportunity for Alaska's North Slope", SPE 93903, 2005.
- Morrow, N.R., Cram, P.J., and McCaffery, F.G. "Displacement Studies in Dolomite with Wettability Control by Octanoic Acid", SPEJ: 221-232, 1973.
- Morrow, N.R., Tang, G., Valat, M. and Xie, X. "Prospects of Improved Oil Recovery Related to Wettability and Brine Composition" Journal of Petroleum Science and Engineering Vol.20: 267-276, 1998.
- Morrow, N.R. and Buckley, J.S. "Improved Oil Recovery by Low-Salinity Waterflooding", SPE Distinguished Author Series Vol.63, May, 2011.
- Pu, H., Xie, X., Yin, P., and Morrow, N.R. "Application of Coalbed Methane Water to Oil Recovery by Low Salinity Waterflooding", SPE 113410, 2008.
- RezaeDoust, A., Puntervold, T., Strand, S., and Austad, T. "Smart Water as Wettability Modifier in Carbonate and Sandstone: A Discussion of Similarities/Differences in the Chemical Mechanisms", Energy Fuels Vol. 23: 4479-4485, 2009.
- RezaeDoust, A., Puntervold, T., and Austad, T. "A Discussion of the Low Salinity EOR Potential for North Sea Sandstone Field", SPE 134459.
- Rivet, S., Lake, L.W., and Pope, G.A. "A Coreflood Investigation of Low-Salinity Enhanced Oil Recovery", SPE 134297, 2010.
- Robertson, E.P. "Low-Salinity Waterflooding to Improve Oil Recovery-Historical Field Evidence", SPE 109965, 2007.
- Salathiel, R.A. "Oil Recovery by Surface Film Drainage in Mixed-Wettability Rocks", Journal of Petroleum Technology Vol.25: 1216-1224, 1973.
- Secombe, J., Lager, A., Webb, K., Jerauld, G., and Fueg, E. "Improving Waterflood Recovery: LoSalTM EOR Field Evaluation", SPE 113480, 2008.
- Secombe, J., Lager, A., Jerauld, G., Jhaveri, B., Buikema, T., Bassler, S., Denis, J., Webb, K., Cockin, A., and Fueg, E. "Demonstration of Low-Salinity EOR at Interwell Scale, Endicott Field, Alaska", SPE 129692, 2010.
- Sharma, M.M. and Filoco, P.R. "Effect of Brine Salinity and Crude-Oil Properties on Oil Recovery and Residual Saturations", SPE Journal Vol.5: 293-300, 2000.
- Tang, G. and Morrow, N.R. "Salinity, Temperature, Oil Composition and Oil Recovery by Waterflooding", SPE Reservoir Engineering Vol.12: 269-276, 1997.
- Tang, G. and Morrow, N.R. "Influence of Brine Composition and Fines Migration on Crude Oil/Brine/Rock Interactions and Oil Recovery", Journal of Petroleum Science and Engineering Vol.24: 99-111, 1999a.

- Tang, G. and Morrow, N.R. "Oil Recovery by Waterflooding and Imbibition – Invading Brine Cation Valency and Salinity.", SCA – 9911 presented at the International Symposium of the Society of Core Analysis in Golden, Colorado, 1999b.
- Tang, G. and Morrow, N.R. "Injection of Dilute Brine and Crude Oil/Brine/Rock Interactions", In Environmental Mechanics: Water, Mass and Energy Transfer in the Biosphere, No.129: 171-179, 2002.
- Webb, K.J., Black, C.J.J., and Al-Ajeel, H. "Low Salinity Oil Recovery- Log-Inject-Log", SPE 89379.
- Willhite, G.P. "Waterflooding", SPE Textbook Series Vol.3, 1956.
- Yildiz, H.O. and Morrow, N.R. "Effect of Brine Composition on Recovery of Moutray Crude Oil by Waterflooding", Journal of Petroleum Science and Engineering Vol.14: 159-168, 1996a.
- Yildiz, H.O., Valvat, M., and Morrow, N.R. "Effect of Brine Composition on Recovery of an Alaskan Crude Oil by Waterflooding", paper presented at the 47th Annual Technical Meeting of the Petroleum Society in Alberta, Canada, Jun. 10-12, 1996b.
- Zhang, Y. and Morrow, N.R. "Comparison of Secondary and Tertiary Recovery with Change in injection Brine Composition for Crude Oil/Sandstone Combinations", SPE 99757, 2006.
- Zhang, Y., Xie, X., and Morrow, N.R. "Waterflood Performance by injection of Brine with Different Salinity for Reservoir Cores", SPE 109849, 2007.
- Zhou, X., Morrow, N.R., and Ma, S. "Interrelationship of Wettability, Initial Water Saturation, Aging Time, and Oil Recovery by Spontaneous Imbibition and Waterflooding", SPE 35436, 10th Symposium on Improved Oil Recovery, Tulsa, Oklahoma, 1996.